

Title	Annealing of Lattice Defects in Single Crystals of p-Type Germanium
Author(s)	Fukuoka, Noboru
Citation	大阪大学, 1969, 博士論文
Version Type	VoR
URL	<a href="https://hdl.handle.net/11094/2482">https://hdl.handle.net/11094/2482</a>
rights	
Note	

*Osaka University Knowledge Archive : OUKA*

<https://ir.library.osaka-u.ac.jp/>

Osaka University

"Annealing of Lattice Defects in Single  
Crystals of p-Type Germanium."

Noboru FUKUOKA

Submitted as a thesis to the Graduate School of Science of the  
Osaka University in partial fulfillment of the requirements  
for the degree of Doctor of Philosophy.

JUNE 1969

## Contents

<b>Abstract</b>	.....	p. 1
§ 1. Introduction	.....	3
§ 2. Experimental Procedure	.....	15
1) Sample and Irradiation	.....	15
2) Method of Measurement	.....	16
§ 3. Experimental Results	.....	19
1) Isochronal Annealing	.....	19
(a) Gallium-Doped Germanium	.....	19
(b) Indium-Doped Germanium	.....	24
2) Isothermal Heating	.....	27
3) Isothermal Annealing	.....	31
§ 4. Discussions	.....	38
1) Annealing of Stage I (80°K ~ 140°K)	.....	38
2) Annealing of Stage III (220°K ~ 270°K)	.....	43
3) Annealing of Stage V (380°K ~     )	.....	50
§ 5. Conclusion	.....	55
§ 6. Acknowledgments	.....	57

## ABSTRACT

Annealing of radiation-induced defects in germanium single crystals was studied by measuring Hall coefficient and conductivity. The dopant was gallium or indium and the impurity concentration ranged from  $3 \times 10^{13}$  to  $5 \times 10^{15}$  atoms/cm<sup>3</sup>. Irradiation of the samples was made by using 1.5MeV electrons at 77°K and the samples were annealed in a temperature range 77° ~ 400°K. Five annealing stages on gallium-doped sample and four stages on indium-doped sample were observed.

Formation of the trap was evident after irradiation. Positions of the two trapping levels were determined to be  $E_C - 0.16\text{eV}$  and  $E_V + 0.16\text{eV}$  in gallium-doped sample. In the case of indium-doped sample, the position of the shallow trapping level was found to be at about  $E_C - 0.10\text{eV}$ . In stage III, which occurs in the range 220°K to 270°K, the traps were annealed out and the donor density increased. In gallium-doped sample, a donor level at 0.08eV above the valence band increased in density as annealing proceeded.

The effect of the defect charge state on the annealing process was also studied. By illuminating the specimens by visible light during annealing, the traps can be filled or, in other words, the charge state of the defect can be changed from that under annealing in the dark. When defects captured electrons, a defect which was otherwise annealable in a range 80° ~ 140°K (stage I) became more stable and another defect annealable in

stage III in the dark was annealed out at lower temperature. The activation energies of the stage III under various conditions were obtained to be as follows; they are 0.38eV with traps empty and 0.23eV with traps full for gallium doped sample, and 0.69eV with traps empty and 0.15eV with traps full for indium doped sample.

In stage V, which occurred above 380°K, the radiation induced change in Hall coefficient and conductivity was annealed out. Activation energy for the stage was obtained to be 1.2eV for gallium doped sample and 1.6eV for indium doped. Characteristics of the five annealing stages and differences in annealing behaviors between gallium and indium doped sample are discussed leading to proposed annealing models.

The annealing process in stage I is considered to be associated with migrating vacancies. In this stage a vacancy with single plus charge migrates to substitutional impurity with single minus charge and makes [vacancy-impurity (substitutional)] complex with single plus charge. The activation energy of this process was found to be 0.1eV. This activation energy is regarded to be that for the migration of vacancies. The model for stage III is as follows; impurity (interstitial) with double plus charge migrates in this stage and makes association with substitutional impurity atom with single negative charge resulting in an association [impurity (interstitial) · impurity (substitutional)] with double plus charge. These models are consistent with the observations in this investigation as well as those in publications by other authors.

## § 1. Introduction

Many of the important physical properties of solids are strongly influenced by various types of defects. It has been recognized that understanding of relations between defect structure and physical properties as well as the knowledges on interactions of imperfections are very important to a better basic understanding of solids. Lattice defects are introduced by plastic deformation, quenching or irradiation with energetic particles; fast neutrons,  $\alpha$ -particles, high-energy electrons and  $\gamma$ -rays. The production of defects by irradiation has several advantages: The relative amount of damage can be easily controlled. The nature of the defect depends on the type of radiation used. By using proper type of irradiation, damage can be introduced quite homogeneously in the crystal.

Defects, like chemical impurities, introduce localized states into the forbidden energy gap of semiconductors. Depending on the material, these defects may ionize as either donors or acceptors. Since radiation damage to a crystalline lattice may be conceived as randomly distributed interstitial-vacancy pairs in its simplest form, the net effect of bombardment on the carrier concentration will depend on the energy level structure of both types of lattice defects. If the acceptor action of one component of the Frenkel pair is stronger than the donor action of the other component, one would naturally expect the carrier concentration of n-type specimens to decrease

with bombardment and conversion to p-type to occur for sufficiently long exposure. Irradiation by electron beams tends to produce a simple defect by removing an isolated atom from its lattice site to an interstitial position leaving behind a vacancy. This Frenkel defect is the most simple radiation produced defect in semiconductors.

The electrical properties of semiconductors are known to be extremely sensitive to both chemical impurities and structural imperfections in the crystal. Hence the study of radiation induced defects in semiconductors has been of great assistance in obtaining recent understandings of the structure of solids. Since behavior of defects upon annealing provides key to a model of the defect and change in defect configurations is reflected in electrical properties, annealing experiments have played an important role in the proceedings of the study of radiation damage. And yet several questions are left unanswered. These are the followings as some of them are raised by Corbett.<sup>1)</sup>

- (1) At what temperature does the migration of vacancies occur and where do they move to?
- (2) At what temperature does the migration of interstitials occur and where do they move to?
- (3) How much is the activation energy of these annealings?
- (4) What is the annealing process?
- (5) What is the role of impurity atom in annealing process?
- (6) What levels are introduced in forbidden band by these defects?

(7) Where is the theory?

There are a number of electrical properties which have been used in studies of these problems. The most extensive studies have been made by using Hall coefficient<sup>2)~5)</sup> and conductivity.<sup>6)~8)</sup> The results yield the concentration and mobility of carriers in the crystal. The number of free carriers provides information on the number of acceptors or donors introduced into the lattice and the carrier mobility provides information about the scattering properties of the defects which reveals the charge state. The minority carrier lifetime,<sup>9)</sup> photoconductivity, electron spin resonance<sup>10)</sup> and optical absorption spectra<sup>11)~14)</sup> are also studied by many investigators.

The fact that the annealing behavior of the radiation-induced changes in carrier concentration and mobility is dependent on species of dopant was first reported by Brown et al.<sup>3)</sup> on n-type germanium. They found that antimony-doped material showed considerably more recovery in the carrier concentration than arsenic-or phosphorus-doped material when the samples irradiated at 80°K were annealed at 329°K. They also found that the variation in reciprocal mobility could be correlated with the change in carrier concentration for the anneal of antimony-doped samples but not for arsenic-doped samples. These results were interpreted as indicating that defect-impurity complexes are formed more readily for some impurities than for others. The additional evidence for the existence of a defect-impurity



interaction was found by Curtis et al.<sup>15)</sup> They showed that recovery of minority carrier lifetime after irradiation of  $\text{Co}^{60}$  gamma-ray at 308°K was influenced not only by the impurity type but also by impurity concentration in both arsenic-and antimony-doped samples. Hasiguti et al.<sup>16)</sup> reported the effect of impurity on the annealing of carrier concentration of  $\text{Co}^{60}$  gamma-ray irradiated germanium. Saito et al.<sup>17)</sup> reported the impurity type and concentration dependence of the annealing of n-type germanium after gamma irradiation at 77°K.

The full dimensions of the possibilities of defect-impurity interactions and complex formation in silicon are shown by the electron spin resonance studies by Watkins and co-workers.<sup>18) ~24)</sup> Among the identified centers are isolated vacancies, vacancy-oxygen complexes, vacancy-substitutional impurity complexes, divacancies and interstitial impurities. There are indications suggesting the presence of impurity-multivacancy complexes and the migration of interstitial impurity atoms at low temperature. In view of the similarity between silicon and germanium, it would not be surprising to find analogous complexes in germanium.

Less report has been published on study of p-type germanium than n-type. This is possibly caused by the lower carrier removal rate of this material. Yet, some studies on radiation damage of p-type germanium have been reported.

Brown et al.<sup>3)</sup> reported the annealing of defects in p-type germanium after 1.0MeV electron irradiation at 79°K. The results

are as follows: Traps of minority carrier are generated by irradiation. The traps are annealed in a temperature range 200°K to 220°K and are replaced by stable donors. The rate of annealing depends strongly upon whether the traps are full or empty. It is interesting that the traps are removed much more readily when they are filled than when they are empty. The activation energy for the annealing was 0.56eV with traps empty and 0.19eV with traps full. No further annealing was observed until 390°K in their indium-doped samples. The activation energy for the annealing was 2.1eV and almost all of the radiation donors were removed in this stage.

Experiments after electron irradiation at 4.2°K were reported by Whitehouse.<sup>8)</sup> He irradiated degenerate p-type germanium at 4.2°K with 4.5MeV electrons and found a carrier removal rate of  $0.4 \text{ cm}^{-1}$ . N-type germanium had a removal rate 25 times larger under the same conditions. Exposure to infrared light ( $h\nu < E_g$ ) caused a change in conductivity decreasing exponentially with time with two different relaxation times. Two processes (P1 and P2) were also observed during the heating of the specimen after irradiation; One (P1), occurring between 30°K and 90°K and another (P2) between 70°K and 110°K. The former tends to restore the conductivity, and this is observed only after infrared irradiation at 4.2°K, and the latter decreases in conductivity once again. If the specimen was exposed to a short pulse of ionizing radiation after the completion of the

latter process, conductivity was restored virtually to its post-irradiation value and this cyclic behavior could be repeated without appreciable loss of radiation induced donors. The most obvious explanation for the decrease of conductivity during illumination is that minority carriers are released from traps and annihilate holes. However, Whitehouse pointed out that the process P1 might be more complex than the simple refilling of traps and involves atomic motion. He suggested that P1 involved the motion of defects to sinks. The P2 process obeyed second order kinetics and the activation energy was 0.16eV.

Similar experiments were done by Flanagan and Klontz.<sup>4), 5)</sup> They showed that when the irradiated samples were illuminated at 5°K with light of energy less than the band gap, the carrier concentration and the electrical conductivity were observed to decay. This decay could be resolved into two independent exponential decays where the ratio of the long-time constant (Exp. 1) to the short-time constant (Exp. 2) was about 6 to 1. They observed four annealing stages and these occurred in the ranges 40° to 70°K, 100° to 150°K, 200° to 270°K and 380° to 420°K. There were two annealing stages in the 40° to 70°K region, one centered near 50°K and the other around 65°K. The value of the activation energy was 0.05eV for the 65°K stage and 0.04eV for the 50°K stage. These stages did not show impurity dependence. The impurity-dependent behavior occurred in the 100° to 150°K range. The activation energy in

this region was 0.10eV. Following the  $100^\circ \sim 150^\circ\text{K}$  transformation, the so called two state defect appeared. This two state defect was stable below  $80^\circ\text{K}$  and the defect behaved like a long-lived minority carrier trap. The two-state defect broke up near  $200^\circ\text{K}$ . This breakup obeyed first order kinetics and the activation energy was 0.40eV. These results are generally similar to those of Whitehouse,<sup>8)</sup> but in some points they are completely different from each other. These differences are considered to be attributed to the differences in experimental conditions such as energy of bombarding electrons, carrier concentration and time of irradiation. These results were the pioneering works on the annealing of p-type germanium. Recently, drastic progress was made by Whan and her work is worth to review.<sup>11)~14)</sup> Whan observed infrared absorption spectrum of oxygen containing germanium and found a formation of oxygen-vacancy complex at low temperature.<sup>14)</sup> Oxygen-doped germanium was irradiated with 2MeV electrons at  $25^\circ\text{K}$  and  $80^\circ\text{K}$ ,<sup>11)</sup> and it was shown that there was an interaction of oxygen atoms with radiation-induced defects in germanium. Two bands at 719 and  $736\text{ cm}^{-1}$ , which were not present after irradiation at  $25^\circ\text{K}$ , developed on annealing between  $58^\circ\text{K}$  and  $73^\circ\text{K}$  in oxygen-doped germanium. The growth of the  $620\text{ cm}^{-1}$  band and the simultaneous decay of 719 and  $736\text{ cm}^{-1}$  bands near  $120^\circ\text{K}$  suggest that the bands are related and impurity-defect interaction occurs in germanium at lower temperature. She used samples doped with  $\text{O}^{18}$  enriched

oxygen and showed that there was a shift of absorption spectrum in vibrational frequency by the change in mass between  $O^{16}$  and  $O^{18}$ . The results showed that the  $620\text{ cm}^{-1}$  band was associated with negatively charged oxygen-vacancy complex. By analogy to oxygen-defect interactions in silicon, these complexes were considered to be oxygen-vacancy complexes, which was formed as the vacancy moves at  $65^\circ\text{K}$ . Similar experiment was done using neutron irradiated germanium.<sup>12)</sup> In this case, the  $620\text{ cm}^{-1}$  band was detectable after irradiation at  $223^\circ\text{K}$  and developed upon annealing above  $273^\circ\text{K}$ . The results are in contrast to those of electron irradiated specimens. This shift in the temperature was understood as the result of additional vacancies produced by the dissociation of the large defect clusters formed by neutron irradiation.

Electron spin resonance is a powerful tool for the study of the detailed nature of radiation induced defects in semiconductors. From the standpoint of electron spin resonance, germanium is a material less satisfactory than silicon. But some works have been published on the electron spin resonance study of defects in germanium.<sup>25)~28)</sup> Baldwin<sup>25),26)</sup> reported the resonance of the germanium A-centers which were generated in oxygen-doped germanium by 2MeV electron irradiation at  $60^\circ\text{C}$ . He observed another two paramagnetic centers, but the models of the defects were not proposed for the lack of resolved hyperfine structure. Hasiiguti et al.<sup>27)</sup> observed electron spin

resonance spectra on arsenic-doped n-type germanium irradiated with 6MeV electrons at 40°C. They observed  $A_1$ , B and C spectrum. The donor spectrum  $A_1$ , which was not observed after irradiation, emerged at 210°C and recovered its intensity before irradiation at 500°C. The B and C spectrum which were observable after irradiation grew stronger until about 210°C, and then they decayed. The B spectrum decayed completely at 500°C and the C spectrum disappeared at 310°C. They proposed the model of C center which gives the C spectrum. The configuration of the model is arsenic divacancy (As -  $V_2$ ) complex. If an arsenic atom situates at the (1/2, 1/2, 1/2) site of the lattice coordinate, two vacancies are situated at two nearest neighbours i. e. (1/4, 1/4, 3/4) and (1/4, 3/4, 1/4). The energy level of the C state is 0.02 ~ 0.03eV below the conduction band. Electron spin resonance on oxygen free p-type germanium was studied by Trueblood.<sup>10)</sup> He irradiated the sample with 4.5MeV electrons at 77°K and observed the resonance of Ge - P1 center. This center showed some of the characteristics of a long-lived electron trap. When the sample was warmed above 77°K, these traps began to empty and the resonance signal decreased. When the sample is warmed above 220°K, the center lost its trapping property. He did not propose a definite microscopic model of the Ge - P1 center, but the high degree of symmetry of the g tensor suggested that the structure of the defect was simple. The studies of electron spin resonance on the radiation defects

in silicon gave many important results for the study of radiation damage.<sup>18)~24)</sup> Many configurations of the defects were determined by Watkins et al.. These results indicated the Si - A center as arising from a vacancy-oxygen pair and Si - E center as arising from a vacancy-phosphorus pair. Watkins<sup>24)</sup> also observed vacancy and interstitial motion. In p-type silicon, the vacancy spectra disappeared in a 15 minute isochronal anneal at  $\sim 160^\circ$  to  $180^\circ\text{K}$  and in n-type silicon, the vacancy spectrum disappeared in a 15 minute isochronal anneal at  $60^\circ\text{K}$ . He found a spectrum arising from interstitial  $\text{Al}^{++}$  in aluminum-doped silicon irradiated at  $4.2^\circ\text{K}$ . He explained the results as follows. The vacancy-interstitial pair is formed in the silicon lattice by irradiation and interstitial silicon atom migrates through the lattice until trapped by the substitutional aluminum atom. In the trapped state, the silicon atom replaces the substitutional aluminum atom, ejecting it into interstitial site. Similar process were observed in copper-doped n-type germanium irradiated at  $77^\circ\text{K}$  by Hiraki et al..<sup>29), 30)</sup> Mackay and Klontz<sup>31), 32)</sup> proposed the close-pair model<sup>33)</sup> for the  $65^\circ\text{K}$  stage of n-type germanium. The vacancy-interstitial pairs are generated by irradiation and they are stable to  $65^\circ\text{K}$ . In the neighborhood of  $65^\circ\text{K}$ , the close-pairs recombine. But recent information indicates that this model is not correct. Zizine<sup>34)</sup> reported a result of isothermal annealing of n-type germanium after irradiation at  $20^\circ\text{K}$  and found an impurity concentration or dopants dependence of the

annealing rate. This result indicates the dependency of the annealing process on either kind or concentration of impurities. Hence, the close-pair model must be abandoned. Zizine took the view that the annealing rate was influenced by the impurity concentration and proposed that the annealing was the result of long range migration of interstitials to recombine with vacancies. But Mackay and Klontz took the view that annealing rate was influenced by the different nature of the impurity. They proposed the model of 65°K stage, such that the interstitial atom trapped by a group V impurity atom migrates to vacancy near 65°K. Ishino et al.<sup>35)</sup> studied the effect of defect charge state to the annealing of n-type germanium and reported that the defects that captured electrons remained stable until 65°K, but without electrons, the defects were annealed out at 30°K.

The amount of published work on p-type germanium<sup>36)~38)</sup> is small compared to that on n-type germanium,<sup>39)~65)</sup> and a more extensive body of experimental information would be helpful to obtain a better understanding of radiation defects in semiconductors. This study was undertaken to investigate the annealing behavior of gallium-or indium-doped germanium under carefully controlled conditions in an attempt to learn some of the details of the annealing processes which occur in the range 80°K to 400°K. Hall coefficient and conductivity were measured during both isochronal and isothermal anneals after irradiation at 77°K. The effect of impurity type or concentration on the



annealing, the effect of defects charge states on the annealing, the activation energy for various annealing stages, the energy levels observed after the various annealing stages and the process of annealing will be discussed together with proposed annealing models.

## § 2. Experimental Procedure

### 1) Sample and Irradiation

The crystals used in this study were gallium-doped or indium-doped germanium. The gallium concentration of the samples is in the range  $3 \times 10^{13}$  to  $5 \times 10^{15}$  atoms/cm<sup>3</sup> and that for the indium-doped sample is  $8 \times 10^{14}$  atoms/cm<sup>3</sup>. Wafers of 0.3 ~ 0.5 mm in thickness were cut from the single crystals perpendicular to the  $\langle 111 \rangle$  axis. Bridge shaped specimens were cut by an ultrasonic die. After the surface of the specimen was etched with CP - 4, ohmic contacts were made by using indium solder containing 5% lead. The specimen was placed in a slot at one end of a sample holder. The holder is a bakelite stick of dimensions 2 × 12 × 370 mm. The slot where the sample is mounted is covered with copper strip with a small hole allowing the electron beam to enter. Electrical insulation between the sample and the copper strip was provided by a layer of cellulose acetate tape placed on the strip. This arrangement protects the sample from breakage without undue thermal insulation. The Hall coefficient and conductivity were measured over a temperature range from 80°K to 400°K prior to irradiation.

The irradiation was made along a  $\langle 111 \rangle$  axis of the crystal with 1.5MeV electrons from a Van de Graaff accelerator. The beam intensity was  $0.8 \mu\text{A}/\text{cm}^2$  or  $4 \mu\text{A}/\text{cm}^2$ . These specimens were mounted on a float so that they were kept at the surface of

liquid nitrogen regardless of the level of the coolant in the box. These arrangements are shown in Fig. 1. After the irradiation was done to a half of total dose, the sample was turned inside out and the opposite side of the sample was irradiated at residual dose. The total dose of irradiation ranged from  $7.5 \times 10^{14}$  to  $2.6 \times 10^{16}$  electrons/cm<sup>2</sup>. Choice of the total dose was made in connection with the impurity concentration and other requirements of the study.

## 2) Method of Measurement

The nature of radiation-induced defects in p-type germanium was studied with the measurement of Hall voltage and conductivity. The magnitude of the Hall voltage is a measure of the free carrier concentration.<sup>66)</sup> The free carrier concentration is the algebraic sum of the concentration of the various charge centers. A measurement of the carrier concentration gives direct information of the concentration of crystal defects. The Hall coefficient  $R_H$  is related to the carrier concentration for intrinsic material by the relation

$$R_H = \frac{3 \pi}{8ec} \frac{p\mu_h^2 - n\mu_e^2}{(p\mu_h + n\mu_e)^2} \quad (\text{e. s. u}) \quad (1)$$

where  $n$  : the electron concentration

$p$  : the hole concentration

$\mu_e$  : the electron mobility

$\mu_h$  : the hole mobility

$e$  : the charge of electron

For a sample in the extrinsic condition

$$R_H = \pm \frac{3 \pi}{8 e c p_i} \quad (\text{e. s. u.}) \quad (2)$$

where  $p_i$  refers to the concentration of the excess carriers and the sign is + for p-type and - for n-type. Then, the excess carrier concentration is given by

$$p_i = \frac{7.38 \times 10^{18}}{R_L} \quad (\text{cm}^{-3}) \quad (3)$$

where  $R_L$  is Hall coefficient represented by practical unit and it has relation  $R_L = 9 \times 10^{19} R_H$ .

Measurements of the Hall voltage and conductivity were made by using an integrating digital voltmeter, and the magnetic field strength for the Hall measurements was 500 oersted. The temperature of the small furnace used for the annealing was electrically controlled to  $\pm 1^\circ\text{K}$  with a chromel-constantan thermocouple and an electronic controller. The schematic representation of temperature controlled furnace and the block diagram of controlling circuit is shown in Fig. 2. Isochronal anneals of 20 min were made at  $10^\circ\text{K}$  intervals in the range from  $80^\circ\text{K}$  to  $400^\circ\text{K}$ . The reference temperature of all measurements was  $77^\circ\text{K}$ . When filled traps were desired, illumination by a miniature electric bulb was used. When the annealing was carried out in the dark, the sample was cooled down to  $77^\circ\text{K}$  and the Hall voltage and conductivity were measured. Next,

the traps were filled by illumination with visible light and the measurement for the traps full condition was made. When the annealing was carried out in visible light, the measurements at 77°K could be made only for the condition of the filled traps. According to the requirements of the study, isothermal annealings in the dark or in visible light were also made. In this case too, the reference temperature of all measurements was 77°K.

The method of the "heating experiment" is described below. This experiment was undertaken with an intention of determining level position of the trap. It can be determined from the temperature dependence of the rate of thermal release of electrons from the traps. The procedures are as follows: After a sample temperature was set to a predetermined "heating" temperature, the traps were filled by illumination of visible light. The moment of turning off light was taken to be the origin of time scale, and the decrease in hole concentrations and conductivity was measured as a function of time. The heating temperature was at least 10°K lower than that of the proceeding annealing in order to avoid undue annealing of the defect. After the heating experiment checks were made to insure that the heating caused no unwanted annealing.

### § 3. Experimental Results

#### 1) Isochronal Annealing

##### (a) Gallium-Doped Germanium

A study of the 20 minute isochronal anneals in the temperature range 80°K to 400°K was made at 10°K intervals. A typical result of 20 minute isochronal anneals on the carrier concentration of gallium-doped sample is shown in Fig. 3. The initial carrier concentration of this sample was  $2.2 \times 10^{14}/\text{cm}^3$  and it decreased to  $1.5 \times 10^{14}/\text{cm}^3$  after irradiation of  $2.1 \times 10^{15}$  electrons/cm<sup>2</sup>. This indicates that the dominant effect of the 77°K electron irradiation is introduction of net donors.

The annealing was performed in the dark. The curve plotted with black dots was obtained after recooling to 77°K in the dark, while that plotted by circles was obtained at 77°K after illumination by visible light. From this figure, it is evident that there are five annealing stages in this temperature range.

Stage I is in the range 80°K ~ 140°K; stage II is in the 150°K ~ 170°K range; stage III is in the 220°K ~ 270°K range; stage IV is in the 330°K ~ 370°K range; and stage V is above 380°K.

The mobility is calculated from Hall coefficient and conductivity by the relation

$$\mu (\text{cm}^2/\text{volt. sec.}) = |R_L| (\text{cm}^3/\text{coul.}) \cdot \sigma (\text{1/ohm-cm})$$

where  $\mu$  is Hall mobility,  $R_L$  is Hall coefficient and  $\sigma$  is conductivity. The change in mobility during the annealing is shown in Fig. 4.

The carrier concentration decreased in the first stage, or in other words the stage is reverse annealing stage. The stage is considered to be associated with emptying of electron traps since illumination after recooling to 77°K reestablishes the near original value. When the measurement was done after recooling to 77°K in the dark, remarkable decrease in mobility was observed. This indicates that the decrease in hole concentration is accompanied by an increase in scattering center density, which is expected for the release of minority carriers from traps. This sample shows conversion from p- to n-type at the end of this stage (⊙ mark shows the electron concentration), suggesting that this stage is to be interpreted not merely as a release of electrons from the traps but to include additional formation of shallow donor levels by some rearrangement of defects. The type conversion was observed to be more pronounced and to cover a wider temperature range in heavily irradiated specimens.

In stage II, the total donor density decreased and the traps began to disappear. Mobility also recovered.

In stage III, the traps were completely annealed and the donor density increased once again. Mobility with traps empty showed little change in this stage, whereas mobility with traps full decreased until it coincided with that with traps empty.

This suggests that the traps were transformed into stable donors which in their ionized stage scatter carriers as effectively as the former empty traps. Similar isochronal annealings were made on samples containing  $3.1 \times 10^{13}$  and  $3.8 \times 10^{15}$  atoms/cm<sup>3</sup> of gallium. On comparing the isochronal annealing curve of the sample containing  $3.1 \times 10^{13}$ /cm<sup>3</sup> gallium atoms with that in Fig. 3, it is easily understood that this stage is much less pronounced in a crystal with less impurity concentration. The annealing behaviors in the other stages are almost the same as shown in Figs. 3 and 4. The sample of Fig. 3 received  $2.1 \times 10^{15}$  electrons/cm<sup>2</sup> and the other one was irradiated to  $1.5 \times 10^{15}$  electrons/cm<sup>2</sup>. Total irradiation doses for these specimens are not much different. Accordingly the difference in impurity concentrations of these samples is considered to be responsible for the difference in annealing behaviours of stage III. The fact that stage III decreases in importance with decreasing gallium concentration indicates that this stage may have some connection with a gallium-defect complex.

In stage IV an increase in donor concentration or a decrease in acceptor density was observed. In this stage too, type conversion was observed in heavily irradiated specimens.

In stage V annealing of donors seems to be occurring and nearly complete recovery of the hole concentration occurs.

In order to explore the effects of charge states to the



annealing processes, the annealing in visible light and the annealing in the dark were studied. Fig. 5 shows the result of this isochronal annealing. When the sample was annealed in the 80°K ~ 110°K range under illumination in the 1st step, the carrier concentration increased and this can be attributed to the stage II. The temperature where the stage II begins in the dark is about 150°K. It is concluded that the temperature for the stage II was lowered by illumination with visible light. After this step, the annealing in the 80°K ~ 150°K range in the dark was done and the decrease of carrier concentration which has been called as stage I was observed. This suggests that the defect associated with the annealing of stage II becomes unstable when it captures electron.

Fig. 6 shows the result of isochronal anneals in visible light for the stage III. The stage III could not be observed by annealing below 220°K in the dark, but it was observed in the annealing at 200°K under illumination with visible light.

Temperature dependence of carrier concentration was measured after isochronal annealing to 280°K, 330°K and 400°K in the dark as shown in Fig. 7. Position of the radiation-induced donor level can be obtained from the measurement. The level position was determined by the next equation. After irradiation, the carrier concentration  $n_A$  is represented as

$$n_A = N_A - \sum_i N_{Di}^+ \quad (i)$$

where  $N_A$  is the initial carrier concentration,  $N_{Di}$  is the donor concentration generated by irradiation and  $N_{Di}^+$  is the concentration of the donor that loses electron. The relation of  $N_{Di}$  and  $N_{Di}^+$  is

$$N_{Di}^+ = \frac{N_{Di}}{1 + \gamma \exp[(E_F - E_{Di})/kT]} \quad (ii)$$

and

$$E_F = E_V + kT \ln N_V/n_A \quad (iii)$$

where  $E_{Di}$  is the position of the donor level introduced by the defect,  $\gamma$  is the ratio of the statistical weight of the vacant state to that of the occupied state,  $E_V$  is the top of the valence band,  $k$  is Boltzmann constant,  $T$  is the absolute temperature and  $N_V$  is the state number of valence band expressed as

$$N_V = 4.83 \times 10^{15} \times \left(\frac{m_p^*}{m}\right)^{\frac{3}{2}} \cdot T^{\frac{3}{2}} / \text{cm}^3.$$

The number of donors which has not released electrons is put  $N_{Di}^0$ . Then,

$$N_{Di}^0 = N_{Di} - N_{Di}^+ \quad (iv)$$

From the eqs. (i)(ii)(iii) and (iv), the following equation can be deduced;

$$n_A \cdot \frac{N_{Di}^0}{N_{Di}^+} = \gamma N_V \exp.(E_V - E_{Di}) / kT \quad (v)$$

As  $N_V$  is proportional to  $T^{\frac{3}{2}}$ , the position of the donor level

is calculated by the slope of a plot of  $\ln(n_A \cdot \frac{N_{Di}^0}{N_{Di}^+} \cdot T^{-\frac{3}{2}})$  vs reciprocal temperature. When the condition of  $n_A \ll N_A$  is satisfied, the eq. (v) can be written in a familiar form,

$$n_A \propto N_V \exp. (E_V - E_{Di}) / kT . \quad (5)$$

The slope of a plot of  $\ln(n_A T^{-\frac{3}{2}})$  vs reciprocal temperature when  $n_A$  is small enough indicates the energy level. From the curves of Fig. 7, it can be concluded that a donor level at  $E_V + 0.08\text{eV}$  exists after annealing at  $280^\circ\text{K}$ , which cannot be seen after completion of the annealing up to  $400^\circ\text{K}$ . The impurity concentration of this sample was  $1.2 \times 10^{14}$  atoms/cm<sup>3</sup>. In the case of crystal with less impurity concentration,  $5.0 \times 10^{13}$  atoms/cm<sup>3</sup>, the donor level  $E_V + 0.08\text{eV}$  was not observed after annealing to  $250^\circ\text{K}$  where the traps had been annealed out.

#### (b) Indium-Doped Germanium

The result of isochronal anneals on the indium-doped sample is shown in Fig. 8. The specimen was irradiated to the total dose of  $1.5 \times 10^{16}$  electrons/cm<sup>2</sup>. From this figure it is evident that there are four annealing stages in the indium-doped sample. An annealing stage corresponding to the stage IV of gallium-doped sample could not be observed in this case, but a stage corresponding to stage V began at about  $360^\circ\text{K}$ . It is also evident that the difference between curves represented by black dots and circles are caused by trapping.

Fig. 9 shows the result of a series of isochronal anneals repeated alternatively under illumination and in the dark. Successive annealings of  $80^{\circ}\text{K} \sim 100^{\circ}\text{K}$  in the dark,  $110^{\circ}\text{K} \sim 120^{\circ}\text{K}$  in visible light and  $110^{\circ}\text{K} \sim 140^{\circ}\text{K}$  in the dark were performed. The measurements were made at the reference temperature of  $77^{\circ}\text{K}$  after illumination with visible light (with traps full). The 1st step of the annealing curve merely means that the stage I is beginning regularly. When the sample was annealed at  $110^{\circ}\text{K}$  and  $120^{\circ}\text{K}$  under illumination in the 2nd step, the carrier concentration evidently increased and this can be attributed to the stage II. The temperature where the stage II begins in the dark is about  $140^{\circ}\text{K}$ . The difference in the temperature range means that the temperature for the stage II is lowered by illumination with visible light. In other words, for the case of indium doped sample too, the defect associated with the stage II becomes unstable under illumination as was the case for gallium doped. After this process, when the sample was annealed at  $110^{\circ}\text{K}$  and  $120^{\circ}\text{K}$  in the dark again, the carrier concentration decreased. This is stage I. The stage I is observed after annealing at  $120^{\circ}\text{K}$  in visible light. Considering from the fact that the temperature where the stage I is finished is  $120^{\circ}\text{K} \sim 130^{\circ}\text{K}$ , the decrease in carrier concentration by annealing at  $110^{\circ}\text{K}$  in the dark suggests that the defect which is annealed in the stage I in the dark was not annealed in the annealing at  $120^{\circ}\text{K}$  in the light. In other words, the defect is

hardly annealed when it captures an electron.

The result of similar experiments on the stage III is shown in Fig. 10. The stage III could not be observed by annealing to 220°K in the dark, but it was observed at 190°K in the annealing under illumination. When the annealing was carried out in visible light, the stage III was finished at 240°K while it was finished at 270°K in the dark. Isochronal annealing curves of the mobility obtained by annealings under illumination and in the dark indicate that the mobility recovers in the stage where the carrier concentration increases and mobility decreases in the stage where the carrier concentration decreases.

In order to study the effect of impurities in detail, isochronal anneals on specimens of gallium-doped and indium-doped were performed after they were exposed to exactly the same dose  $5.0 \times 10^{15}$  electrons/cm<sup>2</sup>. The gallium-doped sample has the initial carrier concentration of  $1.7 \times 10^{14}$ /cm<sup>3</sup> whereas the indium-doped sample has  $6.0 \times 10^{14}$ /cm<sup>3</sup>. The result is shown in Fig. 11, where unannealed fraction  $f(p)$  is plotted against temperature.  $f(p)$  is represented as

$$f(p) = \frac{p_0 - p_t}{p_0 - p_r}$$

where  $p_0$  is the initial carrier concentration,  $p_r$  is the carrier concentration after irradiation and  $p_t$  is the carrier concentration after annealing. The gallium-doped sample showed reverse

annealing to about 140%, while indium-doped sample went up to about 220%. Considering from the figure shown in Fig. 12, it can be concluded that the stage I of gallium-doped specimen has no dependency on impurity concentration. Hence, the difference in the amount of stage I between these two samples should be attributed to the difference in species of the dopants. The conclusion is that the indium-doped sample shows much pronounced stage I annealing than gallium-doped.

## 2) Isothermal Heating

To explore the position of the trapping level, the experiment of the isothermal heating was done. The electrons being captured at the trapping level can be thermally released to the conduction band, when the sample is heated to an appropriate temperature. The probability that an electron excites thermally to conduction band per second, is given by

$$\omega = \nu \exp ( -E_T / kT ) \quad (6)$$

where  $\nu$  is the frequency to escape from the trap,  $E_T$  is the position of trapping level from the conduction band,  $k$  is the Boltzmann constant and  $T$  is the absolute temperature. The time rate of the excitation of electrons to the conduction band is given by

$$- \frac{dn}{dt} = n \nu \exp ( -E_T / kT ) \quad (7)$$

where  $n$  is the number of electrons being trapped. The following equation can be written from eq. (7);

$$\ln n = \nu t \exp ( -E_T / kT ) .$$

This equation can be deformed as

$$\ln n = \alpha t \tag{8}$$

where  $\alpha = \nu \exp ( -E_T / kT )$ . The position of the trapping level  $E_T$  can be determined from the temperature dependence of the time rate of release of electrons. The results of isothermal heating on gallium-doped sample are shown in Fig. 13. After the sample had been annealed to 150°K, the temperature dependence of the time rate of release of electrons at 125°, 130° and 140°K were observed. It was assumed that no annealing of defects occurred during these heatings. This assumption was justified by confirming that the carrier concentration at 77°K before and after heating experiments coincided within the experimental errors. The ⊗ marks indicate carrier concentrations at 77°K before and after heatings. From this experiment the position of this trapping level was estimated to be 0.16eV below the conduction band. The experimental result which leads to this value is shown in Fig. 14. Fig. 15 shows that the release of electrons from this trap at 140°K could not be observed after annealing to 200°K. This shows that these traps were destroyed after annealing to 200°K. However the curve in Fig. 3 indicates

that trapping centers are still present in the crystal. The temperature where all of the traps disappear is 270°K at the end of stage III. Now the question arises what is the trapping center remaining. Another experiment was made to empty the remaining traps by isothermal heatings at 170°K and 200°K, after the sample was isochronally annealed to 230°K. The results are shown in Fig. 16. When a sample is heated at 170°K after isochronal annealing to 230°K, the carrier concentration of the sample decreased indicating that electrons were released from the deep trap at this temperature. When the same sample was kept at 200°K, no electrons were released from the traps. These observations were confirmed on two samples containing different concentrations of gallium. This is understandable if the position of the Fermi level is lower than that of the trapping level at 170°K and above that position at 200°K. The Fermi level is calculated from the equation

$$p = N_V \exp \{ (E_V - \zeta) / kT \}$$

$$N_V = 4.83 \times 10^{15} \cdot \left( \frac{m_p^*}{m} \right)^{\frac{3}{2}} \cdot T^{\frac{3}{2}} / \text{cm}^3$$

where  $p$  is the carrier concentration,  $\zeta$  is the Fermi level position,  $E_V$  is the top of the valence band,  $k$  is the Boltzmann constant,  $m$  is the mass of free electron,  $m_p^*$  is the effective mass of hole and  $T$  is the absolute temperature. From the position of the Fermi level at these temperatures, the deep level



was concluded to lie in the neighborhood of  $E_V + 0.16\text{eV}$ . After annealing at  $270^\circ\text{K}$ , no electrons were released from the traps by isothermal heating at  $170^\circ\text{K}$  suggesting that the deep traps had been destroyed. This is in good agreement with the result shown in Fig. 3. The existence of these two trapping levels is considered to be consistent with the results obtained by Klontz<sup>4)</sup> and Whitehouse.<sup>8)</sup> Similar heating experiments to those carried out on gallium-doped samples were made to determine the level position of the trapping center on indium-doped samples. After the sample had been annealed to  $150^\circ\text{K}$ , the temperature dependence of time rate of release of electrons at  $110^\circ$ ,  $120^\circ$ ,  $130^\circ$  and  $135^\circ\text{K}$  were observed. Position of the shallow trapping level was found to be  $0.10\text{eV}$  below the conduction band from the slope of lines shown in Fig. 17. As shown in Fig. 18, this trap decreases in strength with isochronal annealing in the range  $150^\circ\text{K} \sim 250^\circ\text{K}$ , and is completely destroyed after annealing to  $270^\circ\text{K}$ . When annealing was done under illumination by visible light, the  $E_C - 0.10\text{eV}$  level was removed at  $230^\circ\text{K}$ . This result is shown in Fig. 19. The temperature where the stage III began was lowered too. These facts suggest that the anneals in this temperature range are greatly affected by charge state of the defects.

On aluminum doped sample, the temperature dependence of the time rate of release of electrons from traps at  $90^\circ$ ,  $95^\circ$ ,  $100^\circ$  and  $110^\circ\text{K}$  were measured after the sample had been annealed

to 130°K and the position of the trapping level was found to be 0.11 eV below the conduction band.

### 3) Isothermal Annealing

In order to investigate each stage in detail, isothermal annealings were made at several temperatures. To study the energy level position on the gallium-doped sample, temperature dependence of carrier concentration after successive annealings at 230°K in the dark was measured. The result is shown in Fig. 20. In a curve plotted after 6 min anneal with traps empty, a step in carrier concentration at about 6 in abscissa is evident. This step was found to be caused by a level at about 0.16 eV above the valence band, and the level is considered to be present prior to the anneal since the step in the curve after 100 min shows little difference from that after 6 min. This level is apparently associated with the trapping level because it was not evident under illumination by visible light and furthermore, it was removed simply by continuing the annealing at the same temperature. The position of this level could also be determined by the isothermal heating experiment after the shallow traps have been removed by annealing at 200°K. The value so obtained agreed exactly with that described above. The decrease of carrier concentration below 100°K is considered to be caused by a donor level lying 0.08 eV above the valence band. Temperature dependence of mobility with traps full after

successive annealings at 230°K is shown in Fig. 21. The decrease in mobility at low temperature can be caused by the ionized  $E_V + 0.08$  eV center. From the figure it is concluded that the density of this level increases as annealing proceeds. As mentioned previously, the  $E_V + 0.08$  eV cannot be detected in the sample that contains little gallium. Hence, the formation of  $E_V + 0.08$  eV level is not necessarily accompanied with the disappearance of  $E_V + 0.16$  eV level. Though in gallium-doped sample a level at  $E_V + 0.08$  eV was observed to form in stage III, a level corresponding to this level was not observed in indium-doped sample. The energy level scheme obtained in this investigation on a gallium-doped sample is summarized in Fig. 22. The trapping levels at  $E_C - 0.16$  eV and  $E_V + 0.16$  eV exist after isochronal anneal to 150°K. The  $E_C - 0.16$  eV level disappears after isochronal anneal to 210°K. After isochronal anneal to 270°K, the  $E_V + 0.16$  eV level disappears and  $E_V + 0.08$  eV level is formed. From Figs. 3 and 8 it is evident that the annealing mechanism of traps in stage III is different between gallium-doped sample and indium-doped sample. In the course of the annealing stage III of the samples containing more than  $10^{14}$  gallium atoms/cm<sup>3</sup>, the carrier concentration did not change with traps empty but decreases with traps full. When the sample was annealed to 270°K, the carrier concentration with traps full coincided with that with traps empty. But, for the sample containing only  $3 \times 10^{13}$  gallium atoms/cm<sup>3</sup>, the carrier concentra-

tion with traps full did not change and that with traps empty increased to coincide each other. Considering these behaviours together with the fact that the  $E_V + 0.08$  eV level was not formed in a sample with small gallium concentration, the decrease in carrier concentration with traps full for the sample with higher gallium concentration can be attributed to the formation of  $E_V + 0.08$  eV level.

For the case of indium-doped sample the carrier concentration of indium-doped sample with traps empty increased and that with traps full decreased. The increase in carrier concentration with traps empty indicates the decrease of total donor density in this stage. The decrease of carrier concentration with traps full suggests the formation of new donor level. The same results were observed on aluminum-doped sample with impurity concentration  $1.2 \times 10^{16}$  atoms/cm<sup>3</sup> in stage III. To study the correlations between annihilation of traps and formation of donors in detail, an isothermal annealing in the dark at 250°K was made on indium-doped sample. The result is shown in Fig. 23. The ratio of the number of disappeared traps to that of newly formed donors in this experiment was calculated to be three to two. This ratio was the same as that obtained for isochronal annealings of the same stage. Another series of work were made to study the activation energies, kinetics and frequency factors of the stages I, III and V. The activation energy can be determined from eq.(9). The time rate of the change in defect con-

centration can be expressed by the simple equation

$$\frac{dn}{dt} = - F(n)K = - F(n)K_0 e^{-E_a/kT} \quad (i)$$

where  $n$  is the fractional concentration of the defect,  $F(n)$  is any continuous function of  $n$ ,  $k$  is the Boltzmann constant,  $T$  is the absolute temperature,  $t$  is annealing time and  $K$  is the characteristic rate constant, which can be separated into a pre-exponential constant  $K_0$  and an exponential involving the activation energy of the process,  $E_a$ . Suppose that the isothermal annealing curves have been determined experimentally at several temperatures on a set of identical samples, i.e., samples containing the same initial concentration of defects  $n_0$ . In this case, eq.(i) is formally integrable to give

$$- \int_{n_0}^{n_1} \frac{dn}{F(n)} = K_0 t e^{-E_a/kT} \quad (ii)$$

Different times and temperatures needed to reach the value  $n_1$  are therefore related by the equation

$$t e^{-E_a/kT} = \text{const.} \quad (9)$$

Then the value of activation energy  $E_a$  can be determined from the slope of the curve  $\ln t$  vs  $1/T$ . From three isothermal annealings made at 85°, 100° and 120°K in the dark, the activation energy for stage I was obtained to be 0.10 eV as shown in Fig. 24. In order to investigate the stage III of gallium-doped sample, four isothermal annealings were made at 230°, 235°, 245° and 250°K in the dark. Fig. 25 shows the temperature dependence

of the time for 50% anneal, and from these data the activation energy was calculated to be 0.38 eV with traps empty. The isothermal annealing curves in visible light are shown in Fig. 26. The parameter  $f(p)$  was calculated from the following formula

$$f(p) = \frac{p_a - p_t}{p_a - p_r}$$

where  $p_a$  is the carrier concentration at the end of the stage,  $p_t$  is the carrier concentration after annealed for time  $t$  and  $p_r$  is the carrier concentration before annealing of the stage. From Fig. 27 the activation energy for the traps full condition was obtained to be 0.23 eV on gallium-doped sample. Similar experiments were made on indium-doped sample. From five isothermal annealings made at 225°, 230°, 235°, 240° and 245°K in the dark, the activation energy for traps empty was obtained to be 0.69 eV as shown in Fig. 28. Four isothermal annealings of indium-doped samples were made at 200°, 205°, 210° and 220°K in visible light. From these data the activation energy was found to be 0.15 eV as shown in Fig. 29. Stage III exhibits markedly different activation energies, depending upon whether the traps are empty or full on gallium-doped or indium-doped samples.

The results of gallium-doped sample in stage V are shown in Figs. 30 and 31. Fig. 30 shows the isothermal annealing curves at 380°, 385°, 390° and 400°K. Fig. 31 shows the

temperature dependence of the time for 50% anneal. The activation energy for the stage V was calculated to be 1.2 eV for gallium-doped sample. Similar isothermal annealings were made at 360°, 365°, 370°, 375° and 390°K, for indium-doped samples, and the activation energy was obtained to be 1.6 eV as shown in Fig. 32.

Another information can be obtained from isothermal anneals as to the nature of the annealing. One of the best clues to determine the nature of the annealing process is the order of the annealing reaction. The order of the annealing reaction is determined from the equation

$$\frac{dp}{dt} = K p^\gamma \quad (10)$$

where  $p$  is the carrier concentration,  $K$  is a constant and  $\gamma$  is the order of the reaction. For a case in which  $\gamma$  is unity, a plot of  $\log p$  vs time for isothermal annealing will give a straight line. For other value of  $\gamma$ , a plot of  $\log p$  vs  $\log$  (time) will yield a straight line of slope  $1/(1-\gamma)$ . The orders of reactions were determined by using eq.(10) for the stages III and V. It was found that the kinetics for the stage III is 1st order and that for the stage V is 2nd order. Another useful clue to determine the model of the annealing is the analysis of the pre-exponential factors. Using the value of activation energy and isothermal annealing curves, the frequency factor  $\nu$  is calculated from the equation

$$\tau = \nu^{-1} \cdot \exp\left(-\frac{E_a}{kT}\right) \quad (11)$$

where  $\tau$  is the relaxation time of annealing,  $E_a$  is the activation energy,  $k$  is the Boltzmann constant and  $T$  is the absolute temperature. The frequency factor for the stage III was calculated to be  $5 \times 10^4$ /sec with traps empty and  $4 \times 10^1$ /sec with traps full for gallium-doped sample, while for indium-doped sample these values are  $1 \times 10^{12}$ /sec with traps empty and 3/sec with traps full. The frequency factor in the stage V is  $1 \times 10^{12}$ /sec on gallium-doped and  $1 \times 10^{18}$ /sec on indium-doped sample. The obtained frequency factors are much different from each other depending on impurities. These results are shown in Table 1. The discussion of pre-exponential factors can be lead to the estimation of number of sinks. This will be discussed later.



#### § 4. Discussions

##### 1) Annealing of Stage I (80°K ~ 140°K)

This work has been undertaken to investigate the annealing behavior of the defects produced by 1.5MeV electron irradiation in p-type germanium. In this work, it was revealed that there are five annealing stages in the temperature range 80° ~ 400°K. Each stage will be discussed separately below.

The obtained informations about stage I can be summarized as follows:

(1) The carrier concentration, conductivity and mobility decreases in the stage and the decreases enhance the radiation induced changes. Namely the stage is reverse annealing.

The results are shown in Figs. 3, 4 and 8. The decrease in carrier concentration and mobility after traps are filled by illumination suggests that new donor level is formed on annealing. The decrease in carrier concentration measured after re-cooling to 77°K in the dark shown by black dots in the figures is mainly due to the thermal release of electrons from the traps. The defect center acting as an effective electron trap should be multiply charged positive. In the simplest case it is assumed to be double charged positive at thermal equilibrium and single charged positive with traps full. Then the hole concentration  $p$  is represented as

$$p_e = n_a + N_A - N_D - 2N_T \quad (\text{traps empty})$$

$$p_f = n_a + N_A - N_D - N_T \quad (\text{traps full})$$

where  $n_a$  is the initial carrier concentration,  $N_A$  is the concentration of radiation induced acceptors occupied by electrons,  $N_D$  is the concentration of radiation induced donors and  $N_T$  is the concentration of traps. Type conversion from p-type to n-type at the end of this stage is considered to be attributed to this donor level and the thermal release of electrons from the traps. This stage corresponds to the stage labeled as 2P by Whitehouse<sup>8)</sup> in his paper. He found that this stage was largely suppressed if the metastable states (traps) were emptied by infrared light with  $h\nu < E_g$ , where  $E_g$  was the energy for the band gap. Upon recooling from 120°K, he also found that the post-irradiation hole concentration could be restored by a short burst of ionizing radiation. This behavior is similar to that shown in Figs. 3, 4 and 8 where the carrier concentration was restored upon illumination by visible light in the temperature range below 140°K. Whitehouse merely reported that the activation energy for the process was 0.16eV. In the present investigation it was established that the phenomenon should be attributed to the thermal release of electrons from traps. The position of the trapping level responsible for the phenomenon was found to be  $E_c - 0.16\text{eV}$  as shown in Fig. 14 which was drawn in the heating experiments. The depth of the trapping level coincides to the value of the activation energy reported by

Whitehouse.

(2) The defect which anneals in the stage I is more stable when it captures an electron.

In order to study the effects of charge states on the annealing processes, the annealing in visible light and the annealing in the dark were made. In the study, it was revealed that the defect which anneals in this stage is more stable when it captures an electron. The results are shown in Figs. 5 and 9. Similar phenomenon has been reported on n-type germanium.<sup>35)</sup> Ishino and Mitchell reported that the defects which captured electrons remained stable until 65°K, while without electrons, they were annealed out at 30°K. This annealing stage at 65°K has been considered to be the recombination of vacancy-interstitial close pairs.<sup>7) 31)</sup> Here, it is to be noted that the 65°K stage in n-type is normal recovery, but the stage I in p-type material is reverse annealing. Hence, the annealing mechanism of the stage I in p-type material need not necessarily be the same as that of the 65°K stage in n-type material.

(3) The change in electrical properties in this stage is larger for indium-doped sample than for gallium-doped. To study the effect of impurities on annealing, isochronal annealings of gallium-doped sample and indium-doped one were made after they were exposed to exactly the same dose. Impurity concentration of the gallium-doped sample was  $1.7 \times 10^{14}$  atoms/cm<sup>3</sup> and that of the indium-doped one was  $6.0 \times 10^{14}$  atoms/cm<sup>3</sup>. On comparing

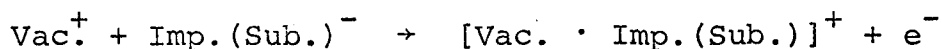
the annealing curves of carrier concentration, it is easily understood that gallium-doped sample showed reverse annealing to 140% as represented by the fraction unannealed defined in section 3-1), while indium-doped went up to about 220%. These results are shown in Fig. 11. Now the question arises what is the cause of the difference in the amount of reverse annealing of these specimens. The amount of reverse annealing for gallium-doped sample is independent of impurity concentration over a range of  $3 \times 10^{13} \sim 5 \times 10^{15}$  atoms/cm<sup>3</sup> as shown in Fig. 12. Hence, the difference in impurity concentration between gallium- and indium-doped samples cannot be the cause. Accordingly the difference should be attributed to some difference in character of gallium and indium atoms. Hirata et al.<sup>67)</sup> studied the annealing of electron irradiated silicon and the difference in annealing behavior was analyzed in terms of impurity atom size. The covalent radius of the gallium atom is 1.26Å, that of indium atom is 1.44Å whereas that of germanium atom is 1.22Å. Here, it is worth while to refer to the work of Whan.<sup>11)</sup> She irradiated an oxygen-doped germanium with electrons of 2MeV at 25°K and found that some association containing vacancy is formed at 60° ~ 70°K. The association was transformed into germanium A-center (vacancy-oxygen complex) at 80° ~ 150°K. The temperature range resembles to that of the stage I of this paper. If the temperature range is that of vacancy migration in germanium, it is reasonable to take vacancy migration into

account on discussing models.

It is very interesting to note that the indium-doped sample whose dopant has larger atom size than gallium shows larger fractional anneal in stage I. Formation of E-center like (vacancy-impurity) association has larger possibility to account for the observed phenomena. It is understandable that the association of large impurity atom and a vacancy is favoured from the standpoint of release of lattice strain.

(4) The activation energy of the stage I was found to be 0.1eV on gallium-doped samples.

Now, a tentative model for the stage I can be proposed. The defect which migrates in the stage I can be assumed to be vacancy<sup>+</sup>. The Vac<sup>+</sup> migrates in the stage I and makes association with impurity(substitutional)<sup>-</sup> resulting in an association [Vac. · Imp.(Sub.)]<sup>+</sup>. This process is expressed in the following formula.



If this model is adopted, the acceptor (Imp.(Sub.)<sup>-</sup>) loses its ability and this causes intrinsic reverse annealing in this stage. This explains the information (1). The information (2) can be understood by considering Coulomb interaction. When the specimen is illuminated by visible light, the vacancy with single positive charge will lose its charge, and the Coulomb interaction between the vacancy and ionized acceptor no more

exists.

From the standpoint of release of lattice strain, the vacancy will prefer to make association with impurity atom of larger size, and this corresponds to the information (3). Thus, this model is consistent with the informations (1), (2), (3) and (4).

In stage II (150°K to 170°K) the total donor density decreased and the trapping level at  $E_c - 0.16\text{eV}$  began to annihilate as shown in Fig. 15. When annealing was made with traps full, this stage occurred at much lower temperature. A model of the defect associated with this annealing stage is not yet known.

## 2) Annealing of Stage III (220°K ~ 270°K)

The annealing of this stage depends on the type of dopant and impurity concentration. Obtained informations on the stage III are summarized as follows:

(1) The amount of this stage is dependent on impurity concentration.

The gallium-doped sample with impurity concentration  $5 \times 10^{13}$  atoms/cm<sup>3</sup> did not show this stage remarkably, and a donor level at  $E_v + 0.08\text{eV}$  was not formed in this sample. This result indicates that the  $E_v + 0.08\text{eV}$  level is associated with a complex defect that contains gallium atom.

(2) For the case of gallium-doped sample, the trapping level at

$E_V + 0.16\text{eV}$  annihilated and a donor level at  $E_V + 0.08\text{eV}$  was formed in stage III. For indium-doped sample, the trapping level at  $E_C - 0.10\text{eV}$  was annealed in this stage. As shown in Figs. 7 and 16, the trap that annihilates in this stage is located at  $E_V + 0.16\text{eV}$  and the donor level at  $E_V + 0.08\text{eV}$  is formed on gallium-doped sample. Neither the  $E_V + 0.08\text{eV}$  level nor the decrease of carrier concentration with traps full was observed for samples with small impurity concentration. This result indicates that the decrease of carrier concentration with traps full is caused by the formation of the  $E_V + 0.08\text{eV}$  level. But the carrier concentration with traps empty did not change. In other words the total donor density does not change in this stage. This behavior can be explained as follows; The trap which is located at  $E_V + 0.16\text{eV}$  and disappears in this stage was transformed into a donor located at  $E_V + 0.08\text{eV}$ . This donor does not exhibit strong trapping properties. On indium-doped sample, the carrier concentration with traps empty increased and that with traps full decreased to coincide with each other. The increase of carrier concentration with traps empty shows the decrease of the total donor density in this stage and the decrease of carrier concentration with traps full indicates the generation of donor level. For the case of indium-doped sample, the  $E_C - 0.10\text{eV}$  trapping level annihilates and a new donor level was formed in this stage. But the position of this donor level could not be

determined.

(3) The defect which anneals in this stage is more unstable when it captures an electron.

Stage III could not be observed by annealing to 210°K in the dark, but it was observed at 190°K in the annealing under illumination with visible light as shown in Figs. 6 and 10. It can be concluded that the defect associated with the stage III is more easily annealed when it captures an electron.

(4) The activation energy for the stage III is 0.38eV with traps empty and 0.23eV with traps full on gallium-doped sample and 0.69eV with traps empty and 0.15eV with traps full on indium-doped sample.

These results are shown in Figs. 25 ~ 32 and Table 1. From the equation (11), the frequency factor was calculated to be  $5 \times 10^4$ /sec for traps empty and  $4 \times 10$ /sec for traps full on the gallium-doped sample. On indium-doped sample the values are  $1 \times 10^{12}$ /sec for traps empty and 3/sec for traps full. The annealing kinetics was found to be first order for both impurities.

Considering from these observations, a tentative model for the defect which is annealed in this stage can be proposed. The requirements for the model are; (a) The defect which is annealed in the stage must be associated with impurity atom. (b) It is transformed into a donor which does not exhibit trapping action. (c) It becomes unstable when it captures electron.



and (d) Annealing kinetics is first order. Most likely defect which accounts for the trapping property is vacancy<sup>++</sup> or interstitial impurity<sup>++</sup>. The existence of impurity(Int.)<sup>++</sup> is expected by an analogy with defect behaviors observed on aluminum-doped silicon<sup>24)</sup> and copper-doped germanium.<sup>29)</sup> If the trap is the Vac.<sup>++</sup> in gallium-doped or indium-doped sample, the position of the trapping level and the value of the activation energy should nearly be the same. But the information (2) and (4) show that the value depends on the dopant impurity. Trueblood<sup>10)</sup> suggested in his electron spin resonance study that the structure of this trapping center is simple. Judging from these considerations, it is deduced that the most probable model for the trapping center is interstitial impurity with double plus charge. If this is the case, what is the sink of the annealing? For first order decomposition, the eq.(10) can be written as

$$\frac{dn}{dt} = -Kn \quad (i)$$

$$\therefore n = A \exp(-Kt) \quad (ii)$$

where n is the number of defects that anneal in the stage and A is a constant.  $\frac{dn}{dt}$  can be written as

$$\frac{dn}{dt} = - \frac{n}{N_0} Z N_s v_0 \exp\left(-\frac{E_a - ST}{kT}\right) \quad (iii)$$

From eqs.(i) and (iii),

$$Kn = \frac{n}{N_0} Z N_s v_0 \exp\left(-\frac{E_a - ST}{kT}\right) . \quad (iv)$$

From eq.(ii), the relaxation time  $\tau$  is represented as

$$\tau = 1/K .$$

Then the eq.(iv) can be rewritten in the next form

$$1/\tau = \frac{1}{N_0} Z N_s v_0 \exp\left(-\frac{E_a - ST}{kT}\right) .$$

The equation can be deformed into the following by using eq.

(11):

$$v_{ob}^{-1} = \frac{N_0}{Z N_s v_0} \exp\left(-\frac{S}{k}\right) . \quad (12)$$

Average number of jumps to reach the sink is

$$N_j = v_0 / v_{ob} \cdot \exp\left(\frac{S}{k}\right) . \quad (13)$$

where  $v_{ob}$  is the observed frequency factor,  $N_0$  is the number of germanium atoms per unit volume,  $Z$  is the number of nearest neighbor sites,  $N_s$  is the number of sinks,  $v_0$  is the attack frequency which is comparable to atomic vibrational frequencies,  $S$  is the entropy of activation and  $N_j$  is the average number of jumps to reach the sink. There are two unknown factor in eq. (12). They are the number of sinks  $N_s$  and the entropy  $S$ . The activation energy and the frequency factor showed larger values for indium-doped specimen than for gallium-doped. This means that the crystals doped with larger covalent radius atoms showed larger value of activation energy and frequency factor than

those doped with smaller sized atoms. This tendency is similar to that observed in the annealing of silicon E-center.<sup>67) 68)</sup> Hirata et al.<sup>69)</sup> showed that the annealings of E-center in silicon are dependent on impurity size and the entropy of activation increases in proportion to the covalent radius of the impurity atom. The entropy factor was experimentally zero for the phosphorous impurity which has almost the same atom size as silicon.

The covalent radius of gallium atom (1.26 $\overset{\circ}{\text{A}}$ ) is not much different from that of germanium atom (1.22 $\overset{\circ}{\text{A}}$ ). Accordingly, when the interaction of the defect and impurity atom is assumed, the entropy factor is considered to be small enough. Thus entropy for gallium-doped specimen is assumed to be zero. Using the values  $v_{ob} = 5 \times 10^4/\text{sec}$ ,  $Z = 4$ ,  $v_o = 1 \times 10^{13}/\text{sec}$ ,  $N_o = 4.5 \times 10^{22} \text{ atoms/cm}^3$  and  $S = 0 \text{ eV/deg}$ , the number of sinks was calculated with eq.(12). This leads to the number of sinks of about  $1 \times 10^{14}/\text{cm}^3$ . The average number of jumps required to reach the sinks is  $2 \times 10^8$ . The activation energy on gallium-doped sample with impurity concentration  $2 \times 10^{15} \text{ atoms/cm}^3$  was the same as that for the impurity concentration of  $2 \times 10^{14} \text{ atoms/cm}^3$ . This indicates that the activation energy is not dependent on impurity concentration. But, the frequency factor is dependent on impurity concentration as discussed below. The observed frequency factor of the sample that contains  $2 \times 10^{15} \text{ impurity atoms/cm}^3$  was  $1.3 \times 10^5/\text{sec}$ . In this case, the concentration of sinks was calculated to be  $1 \times 10^{15}/\text{cm}^3$ . The concentration of sinks for the crystal with

$2 \times 10^{14}$  impurity atoms/cm<sup>3</sup> was calculated to be  $10^{14}$ /cm<sup>3</sup>. If this is the case, the concentration of sinks is of the same order as that of gallium atoms in the crystal. Now a tentative annealing model for the stage III can be proposed. The defect which migrates in this stage is interstitial impurity atom which double plus charge. The gallium(interstitial)<sup>++</sup> makes association with gallium(substitutional)<sup>-</sup> resulting in an association [gallium(Int.) · gallium(Sub.)]<sup>++</sup>. If this model is adopted, the information (1) can be understood easily. Experimental results indicate that the complex cannot be a trapping center any more, but is supposed to be a double donor, because the carrier concentration with traps empty does not change appreciably during stage III. One of the level of this double donor is considered to be at  $E_v + 0.08\text{eV}$ . The results (3) and (4) suggest that the migration energy of the gallium(Int.)<sup>++</sup> is larger than that of gallium(Int.)<sup>+</sup>. For indium-doped sample, the difference between the activation energies with traps empty and full is too large to be reasonably understood as the effect caused by the change in Coulomb interaction between the two components of the complex. The difference in activation energy for different charge states was observed for the migration of vacancy in silicon<sup>24)</sup> and the interstitial atom in n-type germanium.<sup>34)</sup> In n-type germanium, Zizine observed that the migration energy of the neutral interstitial was 0.15eV while

that of a positive interstitial was 0.04eV. The proposed model for the stage III has been thought out on the basis of knowledges on silicon and the main flow with this model is that it requires interstitial gallium to move in the range 220°K to 270°K, whereas interstitial gallium atom in silicon moves near 470°K.<sup>24)</sup> Existence of a shift in annealing temperatures for germanium and silicon was observed on the annealing of A-center. The A-center begins to anneal at 260°K in germanium and at 470°K in silicon.<sup>71)</sup> Hence the difference in temperatures for the migration of gallium atom in germanium and silicon is considered not to be a decisive negative factor of the model.

On indium-doped sample, the same model that the indium(interstitial)<sup>++</sup> migrates and makes a complex with indium(substitutional)<sup>-</sup> is proposed for the annealing of the stage III. From the analogy with gallium-doped sample, the concentration of sinks is considered to be of the same order as that of indium atoms in the crystal. The value of the entropy was calculated to be  $1.2 \times 10^{-3}$  eV/deg for indium-doped sample. The fact that the stage III has the first order kinetics is understandable because the concentration of the sinks is much greater than that of migrating interstitial impurity atom.

### 3) Annealing of Stage V (380°K ~ )

The characteristics of the stage V are as follows :

(1) The carrier concentration and conductivity restore their

preirradiation values in this stage.

(2) The activation energy for the annealing was found to be 1.2eV for gallium-doped sample and 1.6eV for indium-doped sample. Frequency factors obtained are  $1 \times 10^{12}$ /sec for gallium-doped and  $1 \times 10^{18}$ /sec for indium-doped. The annealing kinetics was roughly second order for both impurities.

This stage was also studied by Brown et al.<sup>3)</sup> and Higashinakagawa et al.<sup>70)</sup>. The activation energy obtained by Higashinakagawa for gallium-doped sample was 1.4eV and this value is fairly in good agreement with that obtained in this study. The frequency factors they observed are  $8 \times 10^{14}$ /sec, and this is larger than that in this paper by two orders of magnitude. But the relaxation times  $\tau$  at 400°K in eq.(11) are  $8 \times 10^2$  sec for both cases. Accordingly the difference between the frequency factors can be attributed to the difference in activation energy.

For indium-doped sample, the activation energy obtained was 1.6eV while that obtained by Brown et al. was 2.1eV and that by Higashinakagawa et al. was 1.0eV. Brown et al. made the experiment by using the sample with impurity concentration  $1.5 \times 10^{15}$  atoms/cm<sup>3</sup> and irradiated it at 80°K with 1.0MeV electrons. Higashinakagawa et al. used the sample containing  $7 \times 10^{14}$  impurity atoms/cm<sup>3</sup> and irradiated it with Co<sup>60</sup>  $\gamma$ -ray at 293°K. The cause of the scattered values has not yet been clarified whether it comes from the difference in carrier concentration or the difference in irradiation temperature. No

difference was observed in activation energies of the samples with gallium concentrations  $5 \times 10^{13}$  atoms/cm<sup>3</sup>,  $2 \times 10^{14}$  atoms/cm<sup>3</sup> and  $2 \times 10^{15}$  atoms/cm<sup>3</sup>. The dependency of activation energy and frequency factor on impurity atom size shows similar tendency as that in the case of silicon.<sup>69)</sup> The cause of the large frequency factor  $1 \times 10^{18}$ /sec for indium-doped sample can be explained as follows : The crowding of the lattice by the oversized atom could be relieved by the thermal expansion of the lattice. The activation energy  $E_o$  is represented as

$$E_o = E_a - ST \quad (14)$$

where  $E_a$  is the observed activation energy,  $S$  is the entropy of activation and  $T$  is the absolute temperature. The eq.(11) can be written as

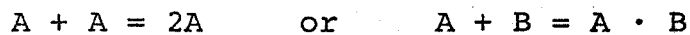
$$\begin{aligned} \tau &= \nu^{-1} \exp\left(\frac{E_o + ST}{kT}\right) \\ &= \nu_1^{-1} \exp\left(\frac{E_o}{kT}\right) \end{aligned}$$

$$\nu_1 = \nu \exp\left(-\frac{S}{k}\right) \quad (15)$$

where  $\tau$  is the relaxation time of annealing,  $\nu$  is the observed frequency factor,  $\nu_1$  is the attack frequency and  $k$  is the Boltzmann constant. If the entropy  $S$  is larger for the larger sized impurity atom, the entropy for indium-doped sample will be large. The entropy  $S$  is calculated with the equation

$$-\frac{dp}{dt} = \frac{Z v_0 p^2}{N_0} \exp\left(-\frac{E_a - ST}{kT}\right) \quad (16)$$

where  $Z$  is the number of nearest neighbor sites,  $p$  is the defect concentration and  $N_0$  is the number of germanium atoms per  $\text{cm}^3$ . The value of the entropy for gallium-doped germanium is  $1.6 \times 10^{-3}$  eV/deg and that for indium-doped germanium is  $2.5 \times 10^{-3}$  eV/deg. Since the value of the entropy is considerably large, large value of the observed frequency factor  $1 \times 10^{18}$ /sec for indium-doped sample is not too surprising. The value of  $v_1$  for indium-doped sample is  $1 \times 10^6$ /sec and that for gallium-doped sample is  $1 \times 10^4$ /sec. Since the annealing kinetics is second order, the annealing process should be either



where  $A$  and  $B$  are defects that anneal in this stage. The isothermal annealing curves were carefully examined and the dependency of the annealing kinetics on each specimens was revealed. The annealing did not exactly obey the second order kinetics for all samples. This result indicates that the annealing kinetics depends on the impurity concentration or the total dose of irradiation. If this is the case, the annealing process will be the association of different defects, namely  $A + B$ . Since a single vacancy and a single interstitial atom in germanium migrate at temperatures far below this stage, this anneal-



ing stage is presumably due to the breakup of the remaining radiation defects.

Considering from the results (1), (2) and the discussions on the entropy and kinetics, there is a large possibility that the dissociation of the [impurity(substitutional)·vacancy] complex is occurring and the vacancy annihilates at the [impurity(Int.)·impurity(Sub.)] complexes.

## § 5. Conclusion

Isochronal and isothermal annealings of irradiated germanium single crystals containing gallium or indium were studied in the temperature range  $80^{\circ} \sim 400^{\circ}\text{K}$ . Five annealing stages for gallium-doped crystal and four annealing stages for indium-doped one were observed.

The stage I was observed in a temperature range  $80^{\circ}\text{K}$  to  $140^{\circ}\text{K}$ . The defect which anneals in the stage was found to be more stable when it captured an electron. The amount of change in carrier concentration by this stage was larger for indium-doped sample than for gallium-doped. Judging from these observations together with other results, the following model for the stage was deduced : The defect which migrates in the stage is  $\text{Vac}^+$ . The  $\text{Vac}^+$  migrates and makes association with  $\text{Imp. (Sub.)}^-$  resulting in an association  $[\text{Vac.} \cdot \text{Imp. (Sub.)}]^+$ . The activation energy for the process was found to be  $0.1\text{eV}$ . This activation energy is regarded to be that of the migration of vacancies.

The annealing behavior of the stage III which occurs in the range  $220^{\circ}\text{K} \sim 270^{\circ}\text{K}$  is strongly dependent on the type and concentration of the dopants. In this stage all of the radiation induced traps were destroyed. The position of the two trapping levels was determined. For the case of gallium-doped crystal the shallow trap is located at  $E_c - 0.16\text{eV}$  and the deep trap is located at  $E_v + 0.16\text{eV}$ . The shallow trap disappeared

after isochronal anneal to 210°K. The deep trap at  $E_V + 0.16\text{eV}$  was destroyed and a donor level at  $E_V + 0.08\text{eV}$  was formed by the end of the stage. The defect which annealed in the stage III was more stable when it captured an electron. The activation energy for the stage was found to be 0.38eV with traps empty and 0.23eV with traps full. For the case of indium-doped sample the shallow trapping level at  $E_C - 0.10\text{eV}$  was destroyed in the stage. The activation energy was found to be 0.69eV with traps empty and 0.15eV with traps full. The samples containing the dopant with larger atom size showed larger values of activation energy and frequency factor than those containing smaller sized dopant. Considering from the experimental evidences, it was concluded that the defect which anneals in the stage is an interstitial impurity atom with double plus charge acting as a trapping center. The sink for the migrating interstitial impurity atom was concluded to be substitutional impurity atom with single negative charge.

In stage V which occurred above 380°K, both the carrier concentration and mobility restored their preirradiation values. The activation energy was found to be 1.2eV for gallium-doped samples and 1.6eV for indium-doped. The large frequency factor of the order of  $10^{18}$ /sec for indium-doped sample is not too surprising when it is discussed together with the entropy factor.

## § 6. Acknowledgments

The author would like to express his sincere thanks to Professor Haruo Saito, for his discussions and encouragements. The helpful suggestions and advices of Professor Mitsuji Hirata and Professor James H. Crawford, Jr. of the University of North Carolina are gratefully acknowledged. He is grateful to Messrs Hironori Hattori and Yukichi Tatsumi for their contributions experimental works.

Heartful thanks are due to Dr. Yota Nakai and Mr. K. Matsuda of the Osaka Laboratory, Japan Atomic Energy Research Institute, without whose kind help in irradiation experiments this work would have been impossible. Thanks are also extended to Miss Junko Hirai for her assistance on the typewriting of this thesis.

## References

- 1) J. W. Corbett, Proceedings of the Santa Fe Conference on Radiation Effects in Semiconductors : Radiation Effects in Semiconductors (Plenum Press, New York, 1968) p. 3.
- 2) G. W. Gobeli, Phys. Rev. 112, 732 (1958).
- 3) W. L. Brown, W. M. Augustyniak, and T. R. Waite, J. Appl. Phys. 30, 1258 (1959).
- 4) E. E. Klontz and T. M. Flanagan, Bull. Am. Phys. Soc. 10, 1199 (1965).
- 5) T. M. Flanagan and E. E. Klontz, Phys. Rev. 167, 789 (1968).
- 6) J. W. Cleland, J. H. Crawford, Jr., K. Lark-Horovitz, J. C. Pigg and F. W. Youngs, Jr., Phys. Rev. 84, 861 (1951).
- 7) J. W. Mackay and E. E. Klontz, J. Appl. Phys. 30, 1269 (1959).
- 8) J. E. Whitehouse, Phys. Rev. 143, 520 (1966).
- 9) W. L. Brown, R. C. Fletcher and K. A. Wright, Phys. Rev. 96, 834 (1954).
- 10) D. L. Trueblood, Phys. Rev. 161, 828 (1967).
- 11) R. E. Whan, Phys. Rev. 140, A690 (1965).
- 12) R. E. Whan, J. Appl. Phys. 37, 2435 (1966).
- 13) R. E. Whan, Proceedings of the Santa Fe Conference on Radiation Effects in Semiconductors : Radiation Effects in Semiconductors (Plenum Press, New York, 1968) p. 195.
- 14) J. F. Becker and J. C. Corelli, J. Appl. Phys. 36, 3606 (1965).

- 15) O. L. Curtis, Jr. and J. H. Crawford, Jr., Phys. Rev. 126, 1342 (1962).
- 16) R. R. Hasiguti and S. Ishino, Proceedings of the Seventh International Conference on the Physics of Semiconductors : Radiation Damage in Semiconductors (Dunod Cie, Paris, 1965) Vol. 3, p. 259.
- 17) H. Saito, J. C. Pigg and J. H. Crawford, Jr., Phys. Rev. 114, 725 (1966).
- 18) G. D. Watkins, Proceedings of the Santa Fe Conference on Radiation Effects in Semiconductors : Radiation Effects in Semiconductors (Plenum Press, New York, 1968) p. 67.
- 19) G. Bamski, J. Appl. Phys. 30, 1195 (1959).
- 20) G. D. Watkins, J. W. Corbett and R. M. Walker, J. Appl. Phys. 30, 1198 (1959).
- 21) G. D. Watkins and J. W. Corbett, Phys. Rev. 121, 1001 (1961).
- 22) J. W. Corbett, G. D. Watkins, R. M. Chrenko and R. S. McDonald, Phys. Rev. 121, 1015 (1961).
- 23) G. D. Watkins, J. Phys. Soc. Japan. 18, 22 (1963).
- 24) G. D. Watkins, Proceedings of the Seventh International Conference on the Physics of Semiconductors : Radiation Damage in Semiconductors (Dunod Cie, Paris, 1965) Vol. 3, p. 97.
- 25) J. A. Baldwin, Jr., J. Appl. Phys. 36, 793 (1965).
- 26) J. A. Baldwin, Jr., J. Appl. Phys. 36, 2079 (1965).

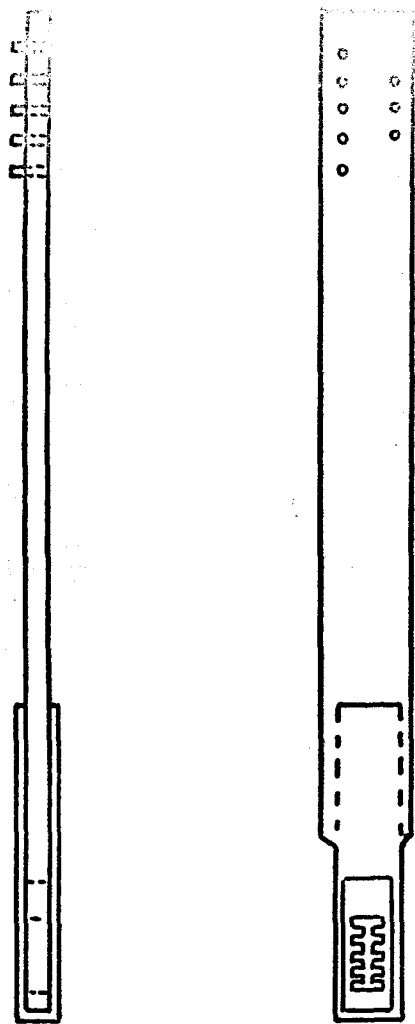
- 27) R. R. Hasiguti, K. Tanaka and S. Takahashi, Proceedings of the Santa Fe Conference on Radiation Effects in Semiconductors : Radiation Effects in Semiconductors (Plenum Press, New York, 1968) p. 89.
- 28) Handy Horiye, J. Appl. Phys. 39, 2146 (1968).
- 29) A. Hiraki, J. W. Cleland and J. H. Crawford, Jr., J. Appl. Phys. 38, 3519 (1967).
- 30) A. Hiraki, J. W. Cleland and J. H. Crawford, Jr., Proceedings of the Santa Fe Conference on Radiation Effects in Semiconductors : Radiation Effects in Semiconductors (Plenum Press, New York, 1968) p. 224.
- 31) E. E. Klontz and J. C. Mackay, J. Phys. Soc. Japan. 18, supplement III, 216 (1963).
- 32) J. W. Mackay and E. E. Klontz, Proceedings of the Santa Fe Conference on Radiation Effects in Semiconductors : Radiation Effects in Semiconductors (Plenum Press, New York, 1968) p. 175.
- 33) G. K. Wertheim, Phys. Rev. 115, 568 (1959).
- 34) J. Zizine, Symposium on Radiation Effects in Semiconductor Components, Toulouse, France, March 1967.
- 35) S. Ishino and E. W. J. Mitchell, Proceedings of the International Symposium on Lattice Defects in Semiconductors, Tokyo, 1966 : Lattice Defects in Semiconductors (Univ. of Tokyo Press, Tokyo, 1968) p. 185.
- 36) N. Fukuoka, H. Saito, H. Hattori and J. H. Crawford, Jr., J. Appl. Phys. 38, 4098 (1967).

- 37) H. Saito, N. Fukuoka, H. Hattori and J. H. Crawford, Jr.,  
Proceedings of the Santa Fe Conference on Radiation Effects  
in Semiconductors : Radiation Effects in Semiconductors  
(Plenum Press, New York, 1968) p. 232.
- 38) H. Saito, N. Fukuoka, H. Hattori and J. H. Crawford, Jr.,  
Proceedings of the International Symposium on Lattice  
Defects in Semiconductors, Tokyo, 1966 : Lattice Defects  
in Semiconductors. (Univ. of Tokyo Press, Tokyo, 1968)  
p. 197.
- 39) W. Shockley and W. T. Read, Jr., Phys. Rev. 87, 835 (1952).
- 40) G. K. Wertheim, Phys. Rev. 109, 1086 (1958).
- 41) O. L. Curtis, Jr., J. Appl. Phys. 30, 1174 (1959).
- 42) O. L. Curtis, Jr. and J. W. Cleland, J. Appl. Phys. 31,  
423 (1960).
- 43) O. L. Curtis, Jr. and J. H. Crawford, Jr., Phys. Rev. 124,  
1731 (1961).
- 44) T. A. Callcott and J. W. Mackay, Phys. Rev. 161, 698 (1967).
- 45) B. G. Streetman, J. Appl. Phys. 37, 3137 (1966).
- 46) B. G. Streetman, J. Appl. Phys. 37, 3145 (1966).
- 47) N. Fukuoka, M. Hirata and H. Saito, Japan. J. Appl. Phys.  
5, 383 (1966).
- 48) R. R. Hasiguti, Japan. J. Appl. Phys. 21, 1927 (1966).
- 49) A. Hiraki, J. Phys. Soc. Japan. 21, 34 (1966).
- 50) F. L. Vook and R. W. Balluffi, Phys. Rev. 113, 62 (1959).
- 51) R. C. Fletcher and W. L. Brown, Phys. Rev. 92, 582 (1953).

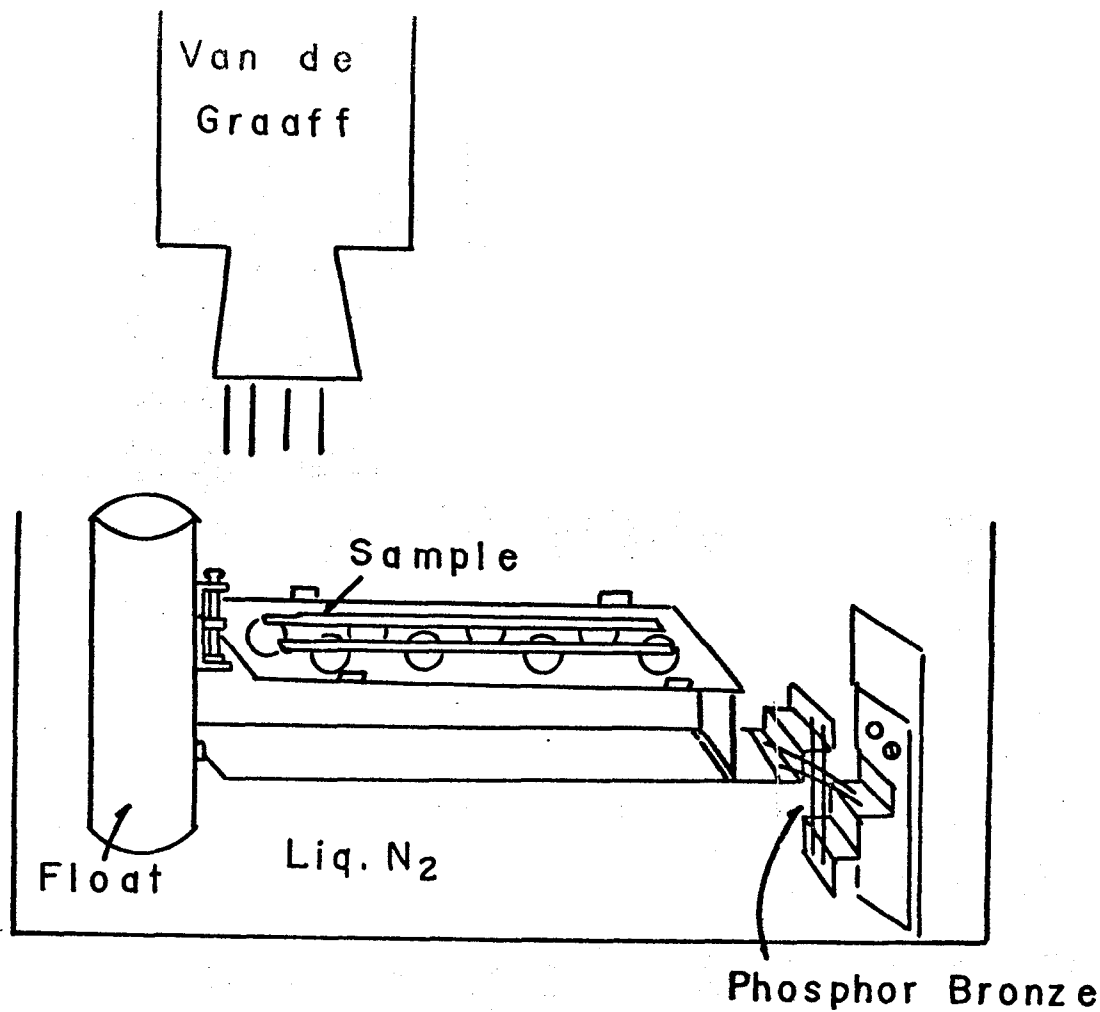


- 52) T. R. Waite, Phys. Rev. 107, 463 (1957).
- 53) F. L. Vook, Phys. Rev. 138, A1234 (1965).
- 54) J. W. Mackay and E. E. Klontz, Proceedings of the Seventh International Conference on the Physics of Semiconductors : Radiation Damage in Semiconductors (Dunod Cie, Paris, 1965) Vol. 3, p. 11.
- 55) V. S. Vavilov, Proceedings of the Seventh International Conference on the Physics of Semiconductors : Radiation Damage in Semiconductors (Dunod Cie, Paris, 1965) Vol. 3, p. 115.
- 56) O. L. Curtis and J. H. Crawford, Jr., Proceedings of the Seventh International Conference on the Physics of Semiconductors (Dunod Cie, Paris, 1965) Vol. 3, p. 143.
- 57) J. E. Fisher and J. C. Corelli, J. Appl. Phys. 37, 3287 (1966).
- 58) S. Ligenza, Proceedings of the Seventh International Conference on the Physics of Semiconductors : Radiation Damage in Semiconductors (Dunod Cie, Paris, 1965) Vol. 3, p. 151.
- 59) A. Scholz and A. Seeger, Proceedings of the Seventh International Conference on the Physics of Semiconductors : Radiation Damage in Semiconductors (Dunod Cie, Paris, 1965) Vol. 3, p. 315.
- 60) W. L. Brown and R. C. Fletcher, Phys. Rev. 92, 591 (1953).
- 61) T. R. Waite, Phys. Rev. 107, 471 (1957).

- 62) M. P. Singh and J. W. Mackay, Phys. Rev. 175, 985 (1968).
- 63) J. H. Crawford, Jr. and J. W. Cleland, J. Appl. Phys. 30, 1204 (1959).
- 64) J. C. Pigg and J. H. Crawford, Jr., Phys. Rev. 135, A1141 (1964).
- 65) J. Zizine, Proceedings of the Santa Fe Conference on Radiation Effects in Semiconductors : Radiation Effects in Semiconductors (Plenum Press, New York, 1968) p. 186.
- 66) W. E. Shockley, Electrons and Holes in Semiconductors (D. Van Nostrand and Company, New York, 1950) p. 204 ~ 217.
- 67) M. Hirata, M. Hirata, H. Saito and J. H. Crawford, Jr., J. Phys. Soc. Japan. 22, 1301 (1967).
- 68) M. Hirata, M. Hirata and H. Saito, Japan. J. Appl. Phys. 5, 252 (1966).
- 69) M. Hirata, M. Hirata, H. Saito and J. H. Crawford, Jr., J. Appl. Phys. 38, 2433 (1967).
- 70) I. Higashinakagawa, S. Ishino, F. Nakazawa and R. R. Hasiguti, Proceedings of the International Symposium on Lattice Defects in Semiconductors, Tokyo, 1966 : Lattice Defects in Semiconductors (Univ. of Tokyo Press, Tokyo, 1968) p. 211.
- 71) R. E. Whan, J. Appl. Phys. 37, 3378 (1966).

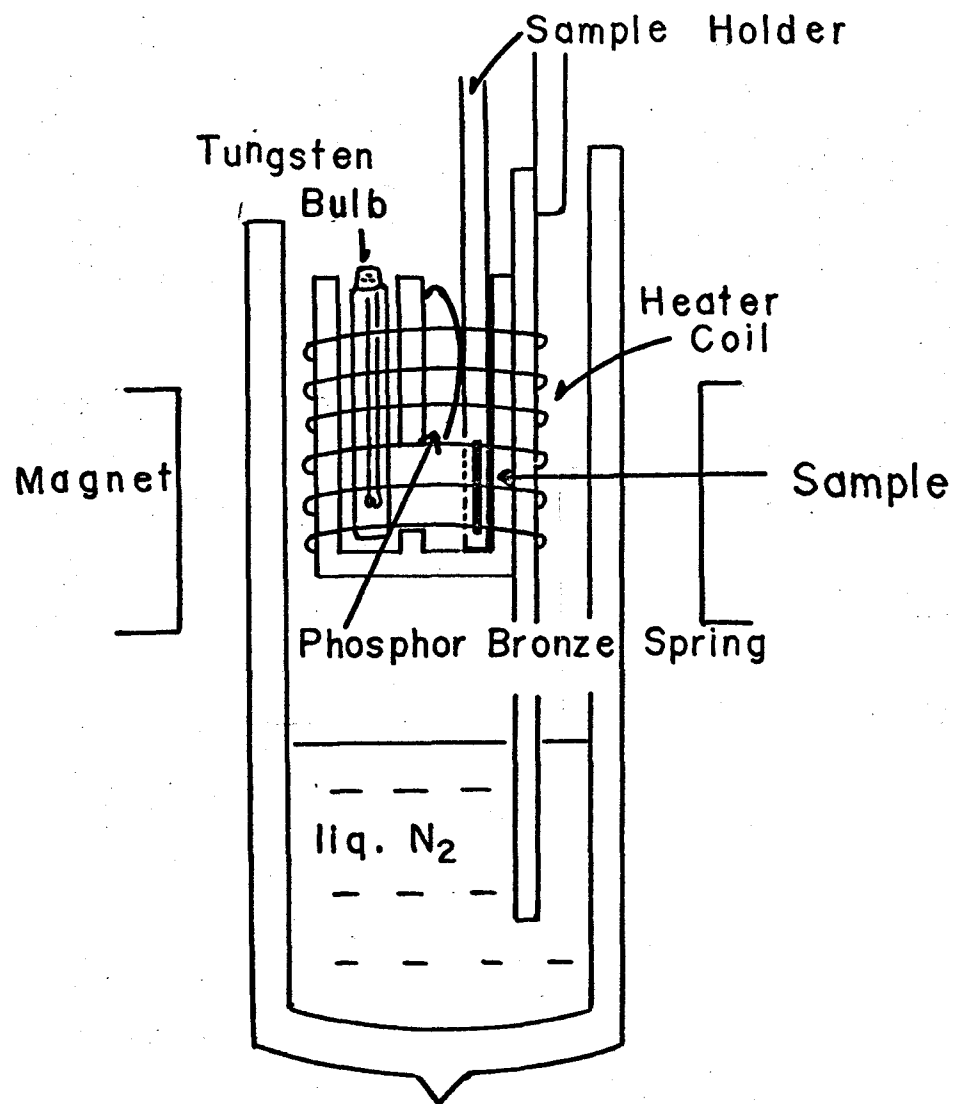


(A)

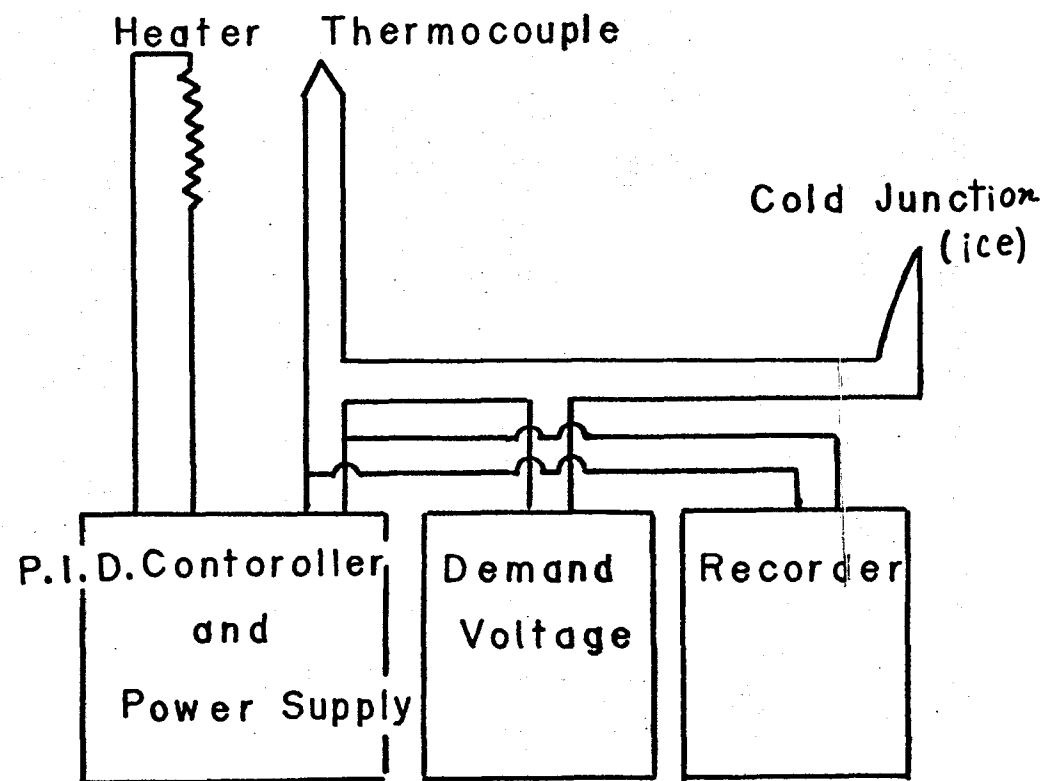


(B)

Fig. 1. Sample holder and schematic representation of the arrangement for irradiation.



(A)



(B)

Fig. 2. Schematic of temperature controlled furnace in measuring position and block diagram of temperature controlling system.

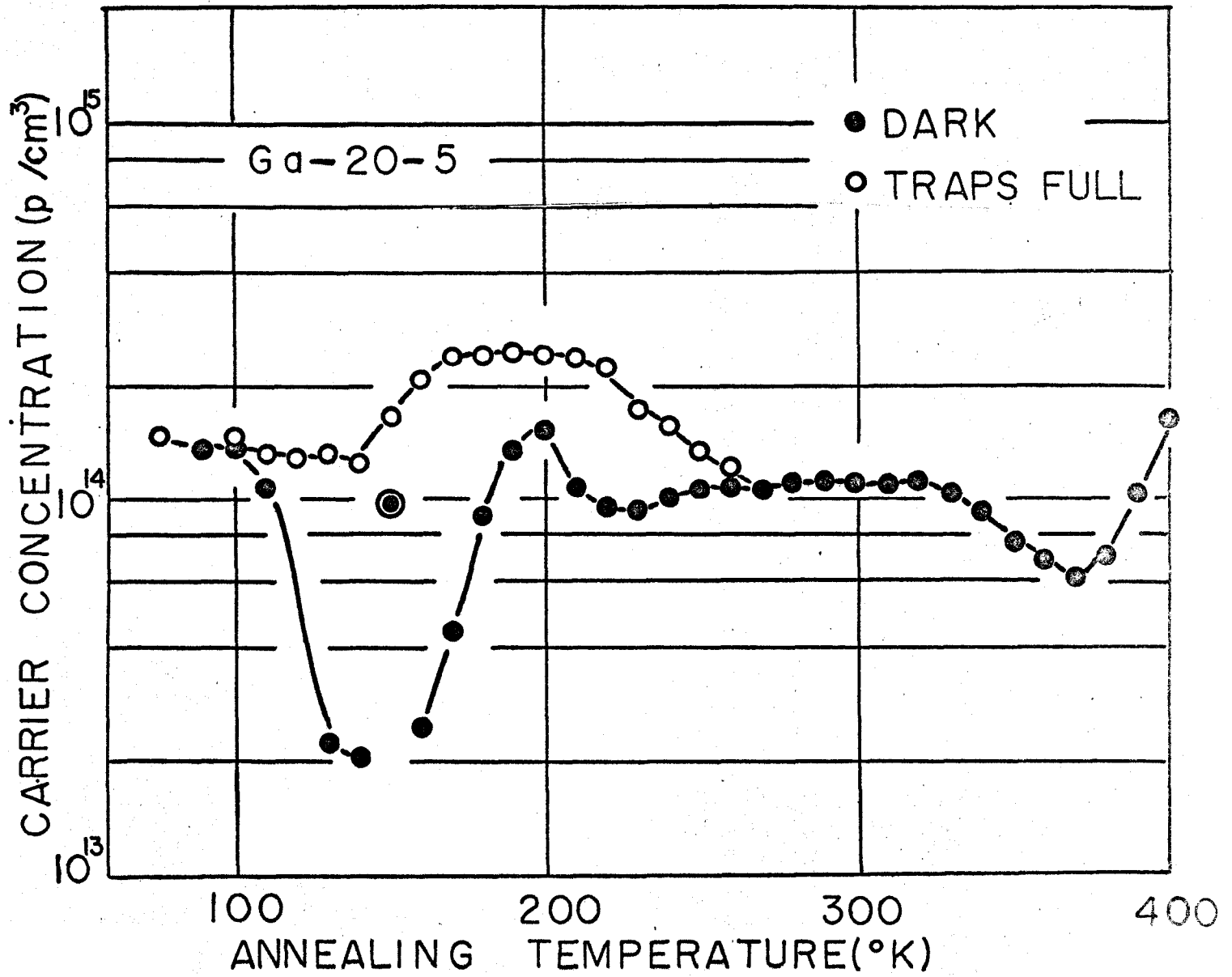


Fig. 3. Result of 20min isochronal annealing in the dark of carrier concentration after irradiation at 77°K.

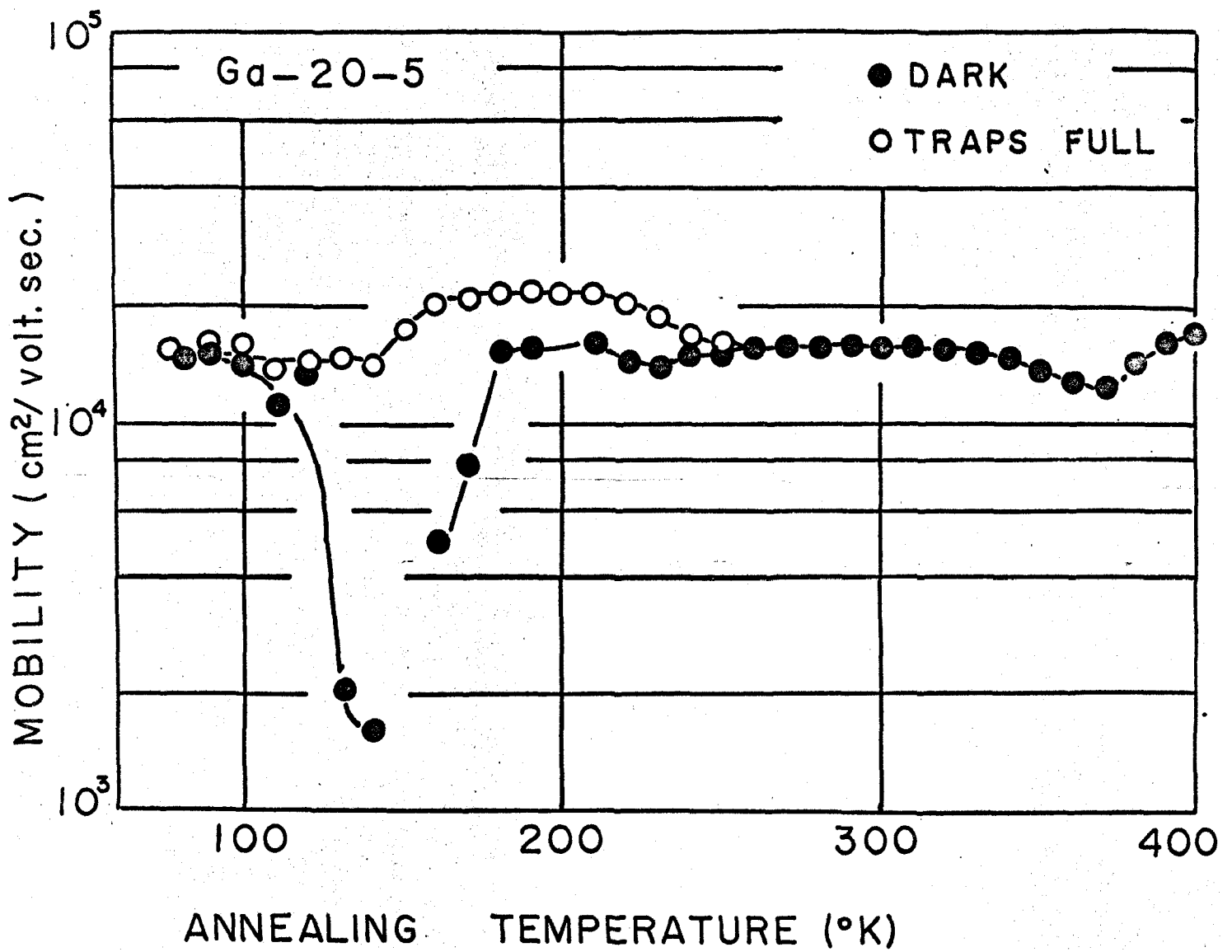


Fig. 4. Result of 20min isochronal annealing in the dark of mobility after irradiation.

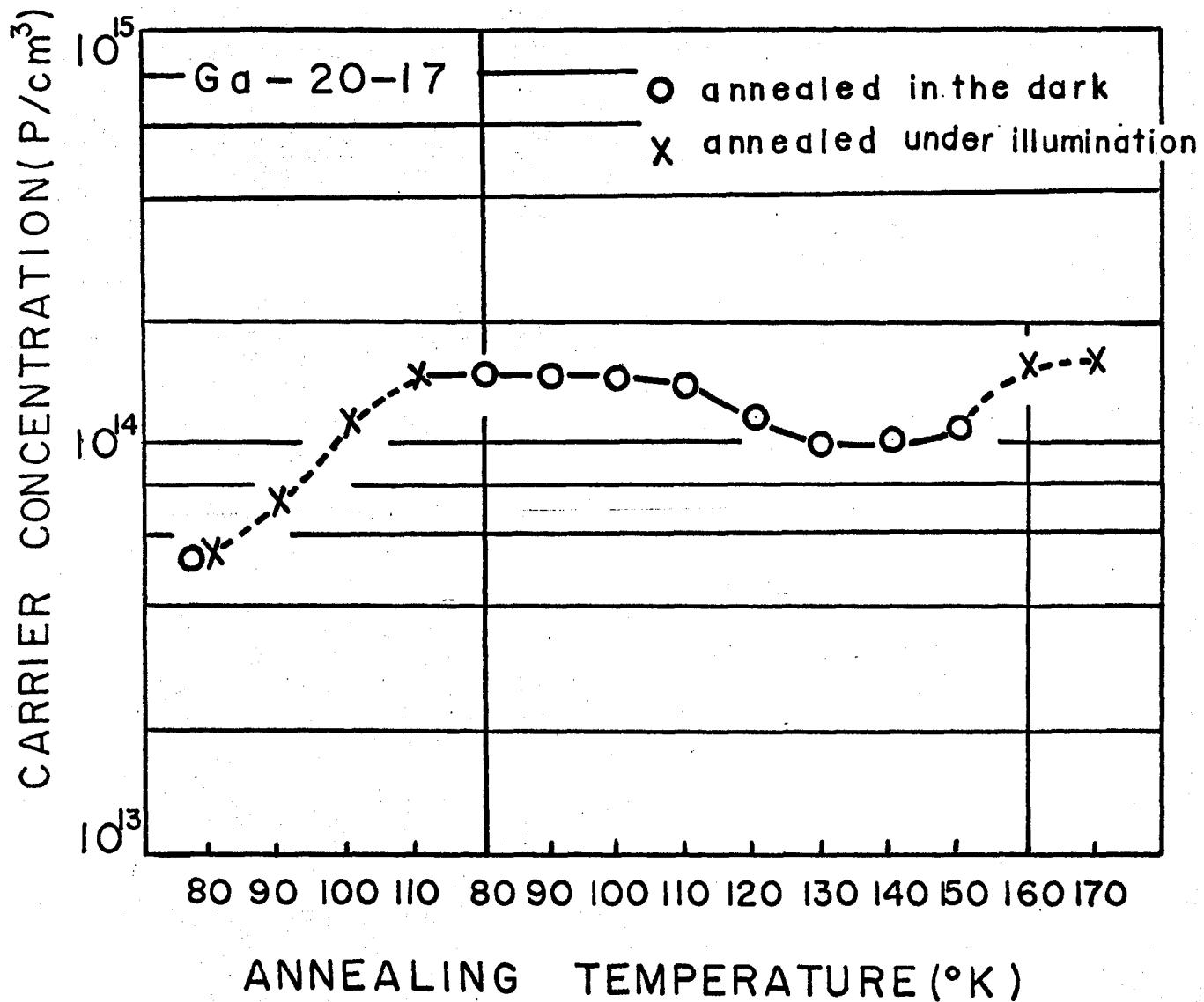


Fig. 5. 20min isochronal annealing curve of gallium-doped crystal. The annealing was carried out alternatively in the dark and under illumination by visible light. The annealing temperature went back and forth after annealing at 110°K.

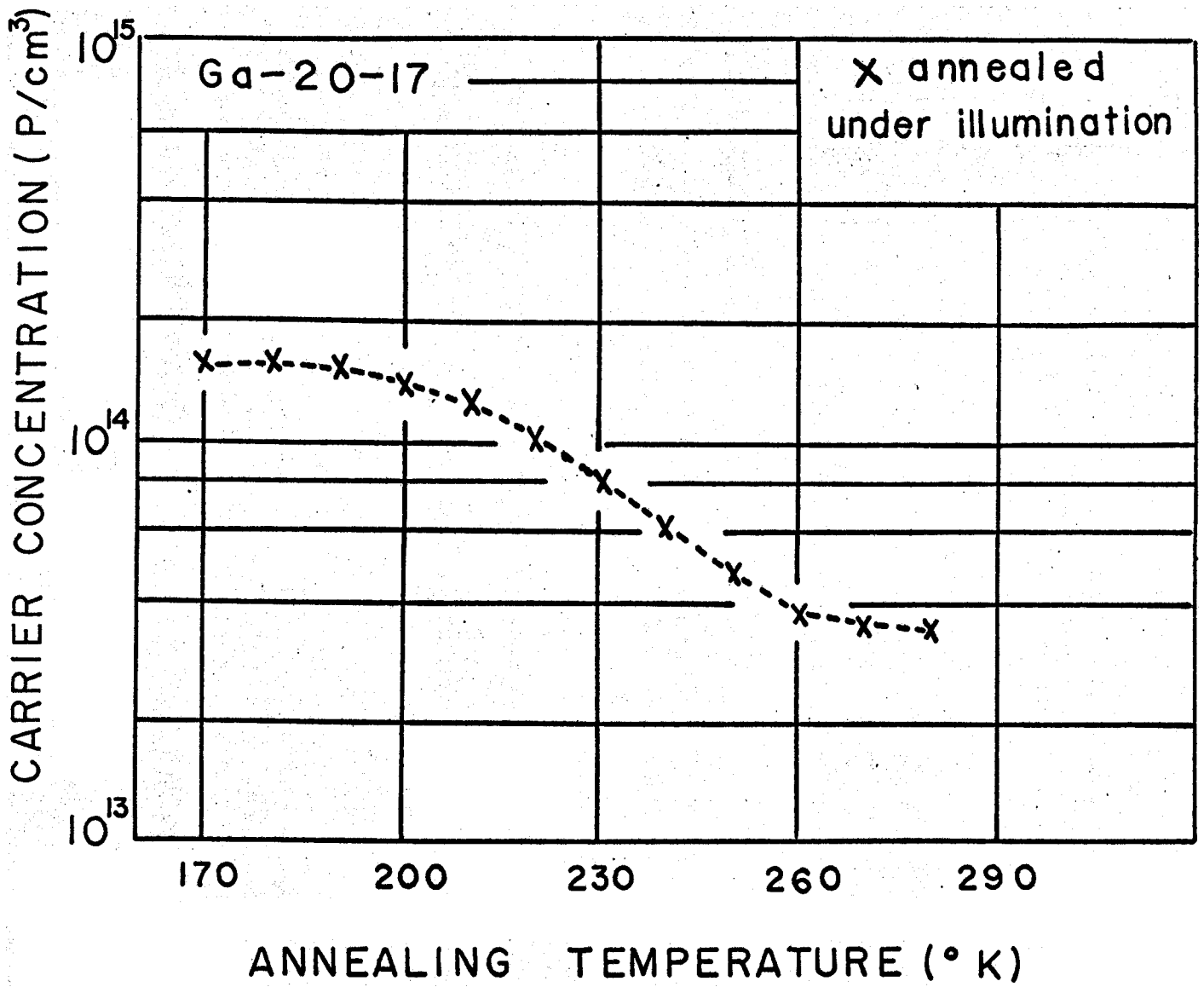


Fig. 6. 20min isochronal annealing in visible light.



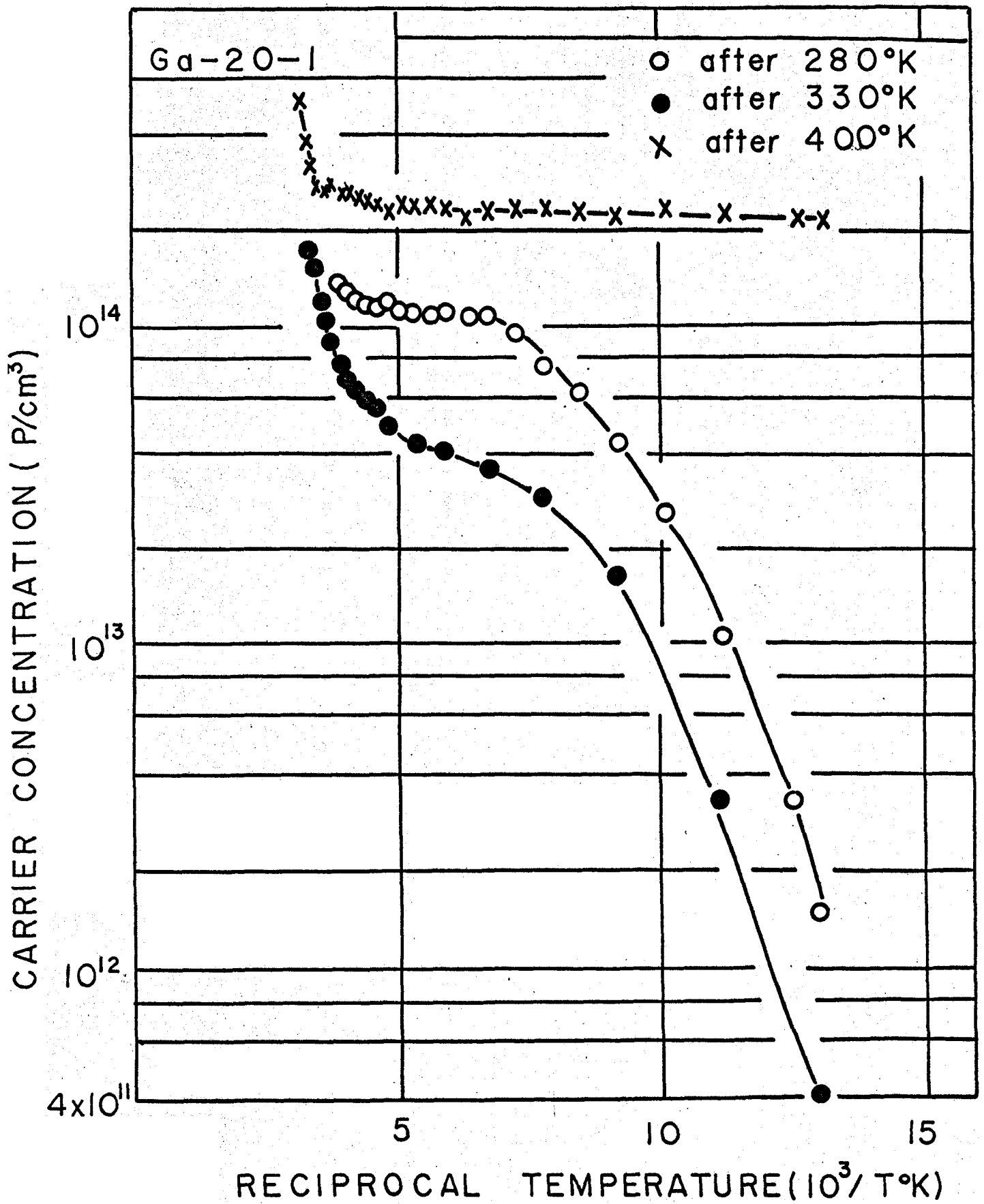


Fig. 7. Temperature dependence of carrier concentration after successive annealings in the dark.

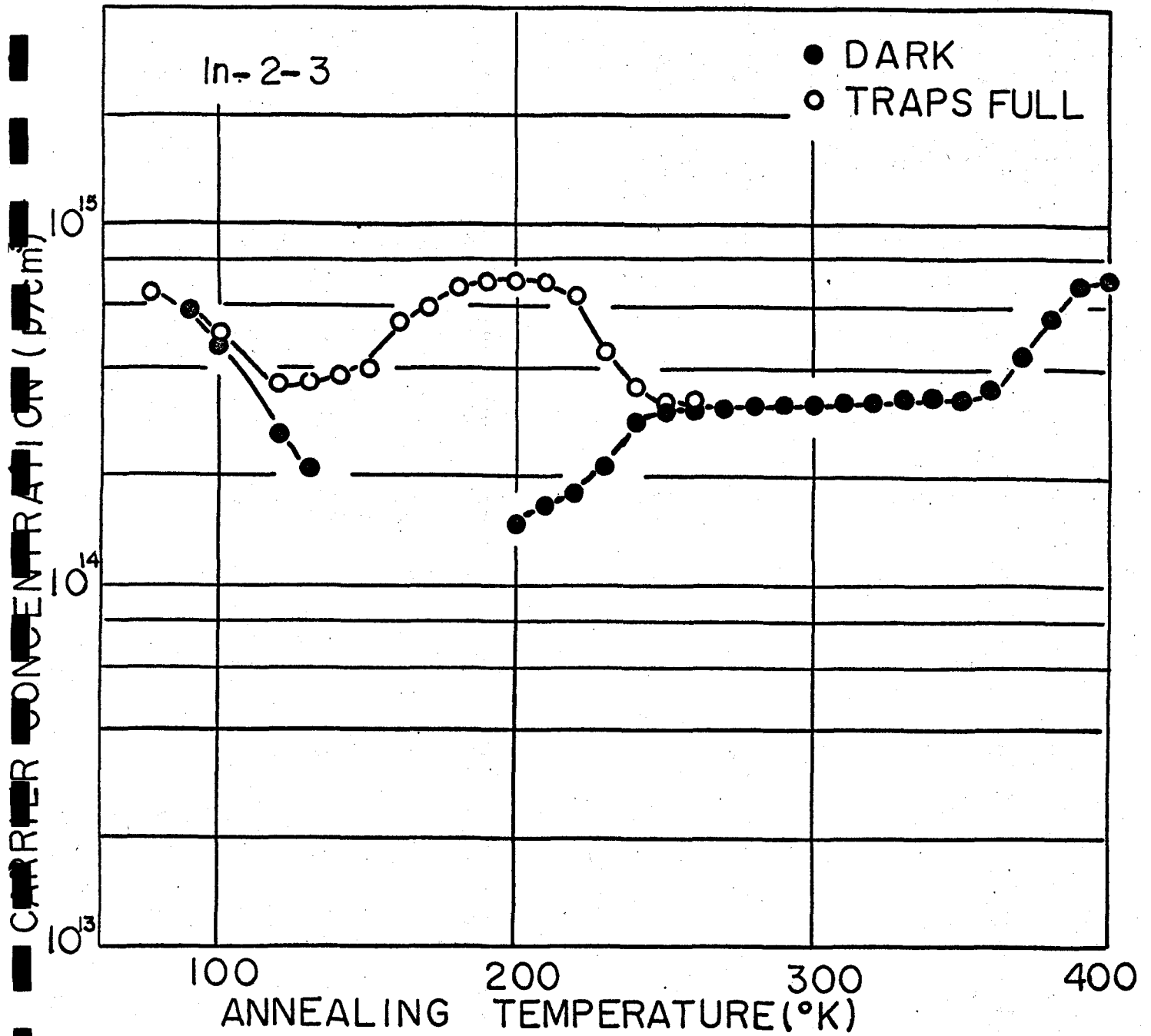


Fig. 8. Result of 20min isochronal anneals in the dark on the carrier concentration in indium-doped sample.

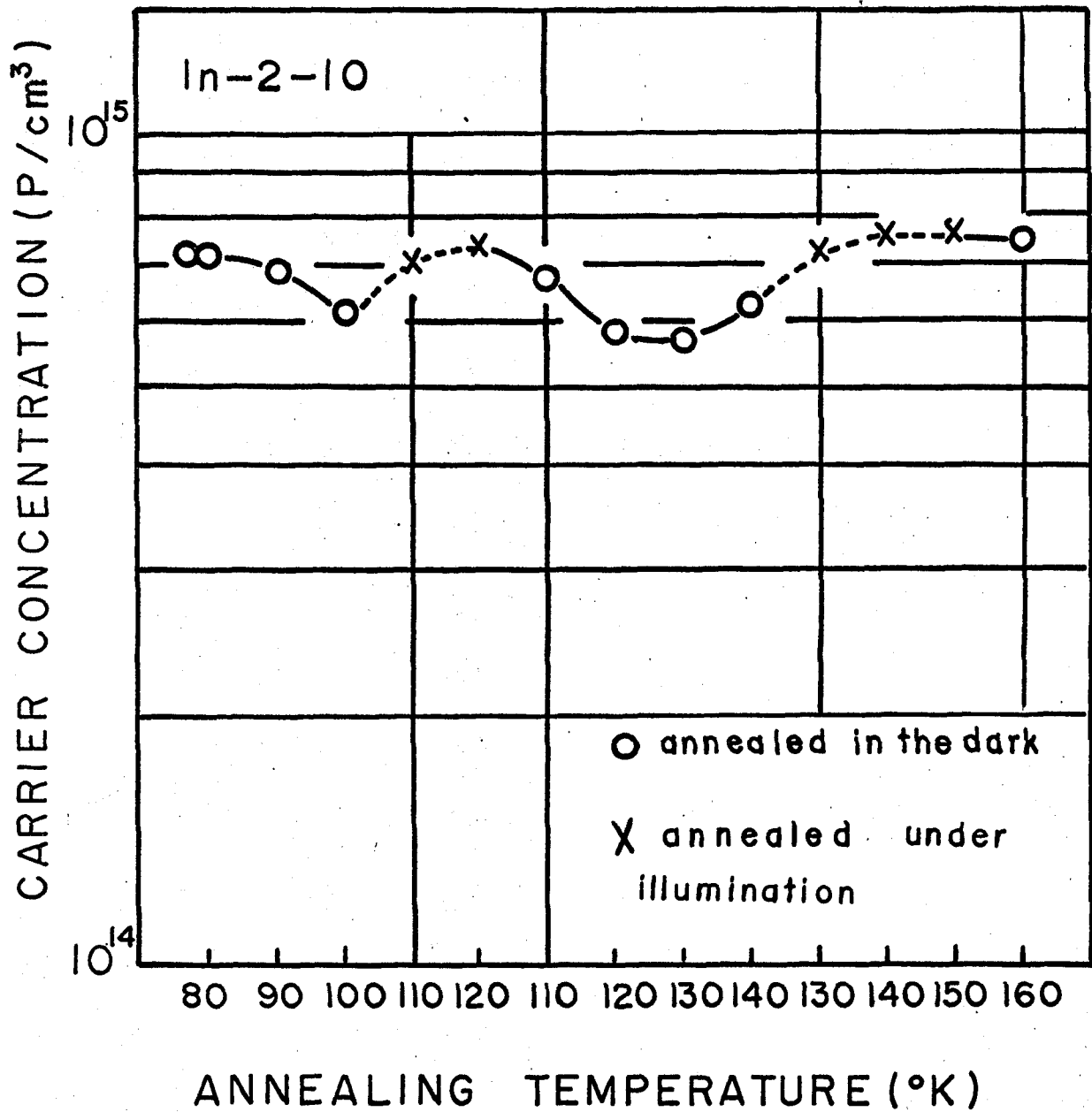


Fig. 9. 20min isochronal annealing curve of indium-doped crystal. The circle shows that the annealing was done in the dark and X mark shows that the annealing was done in visible light.

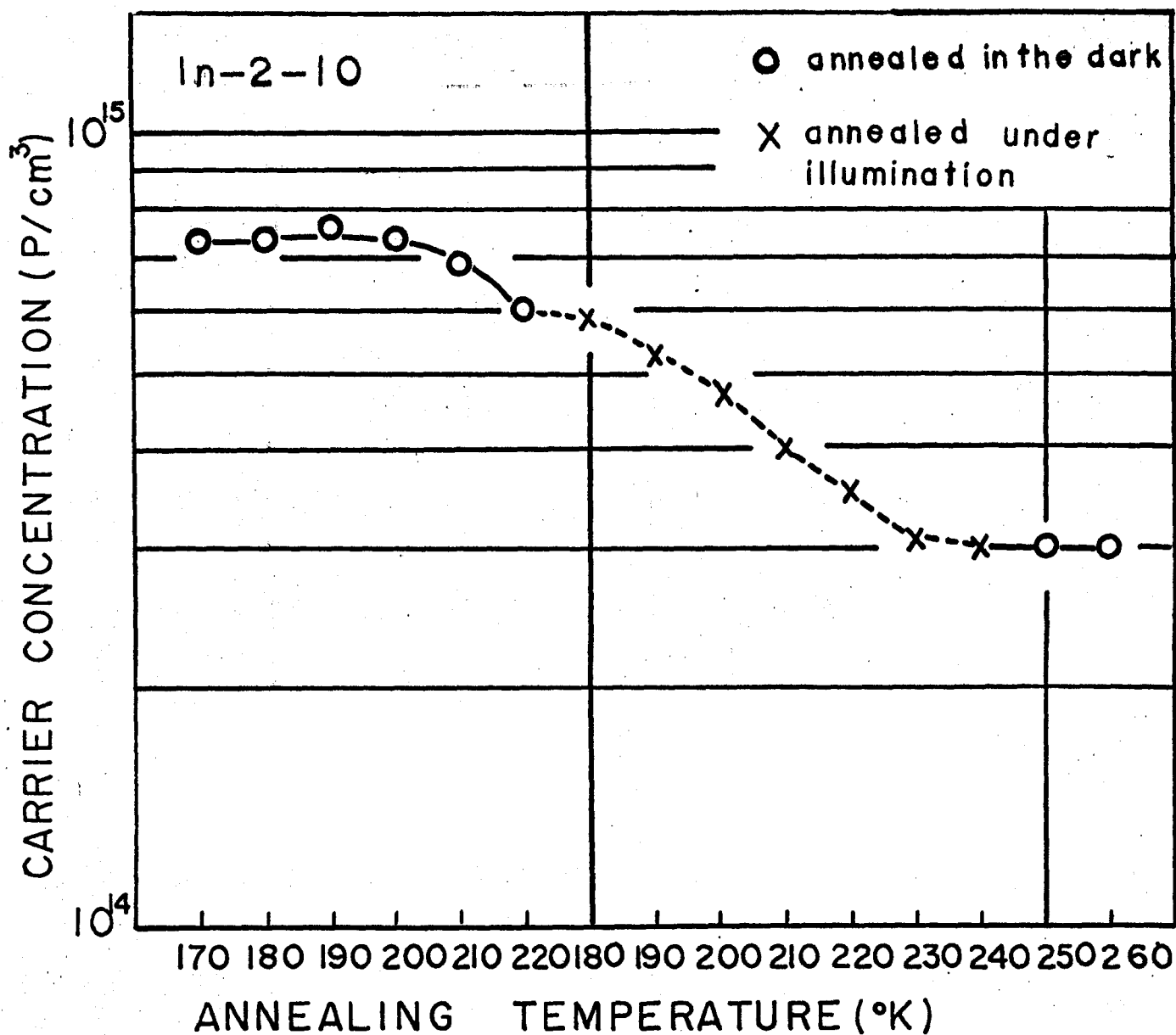


Fig. 10. 20min isochronal annealing curve of indium-doped crystal. The circle shows that the annealing was done in the dark and X mark shows that the annealing was done in visible light.

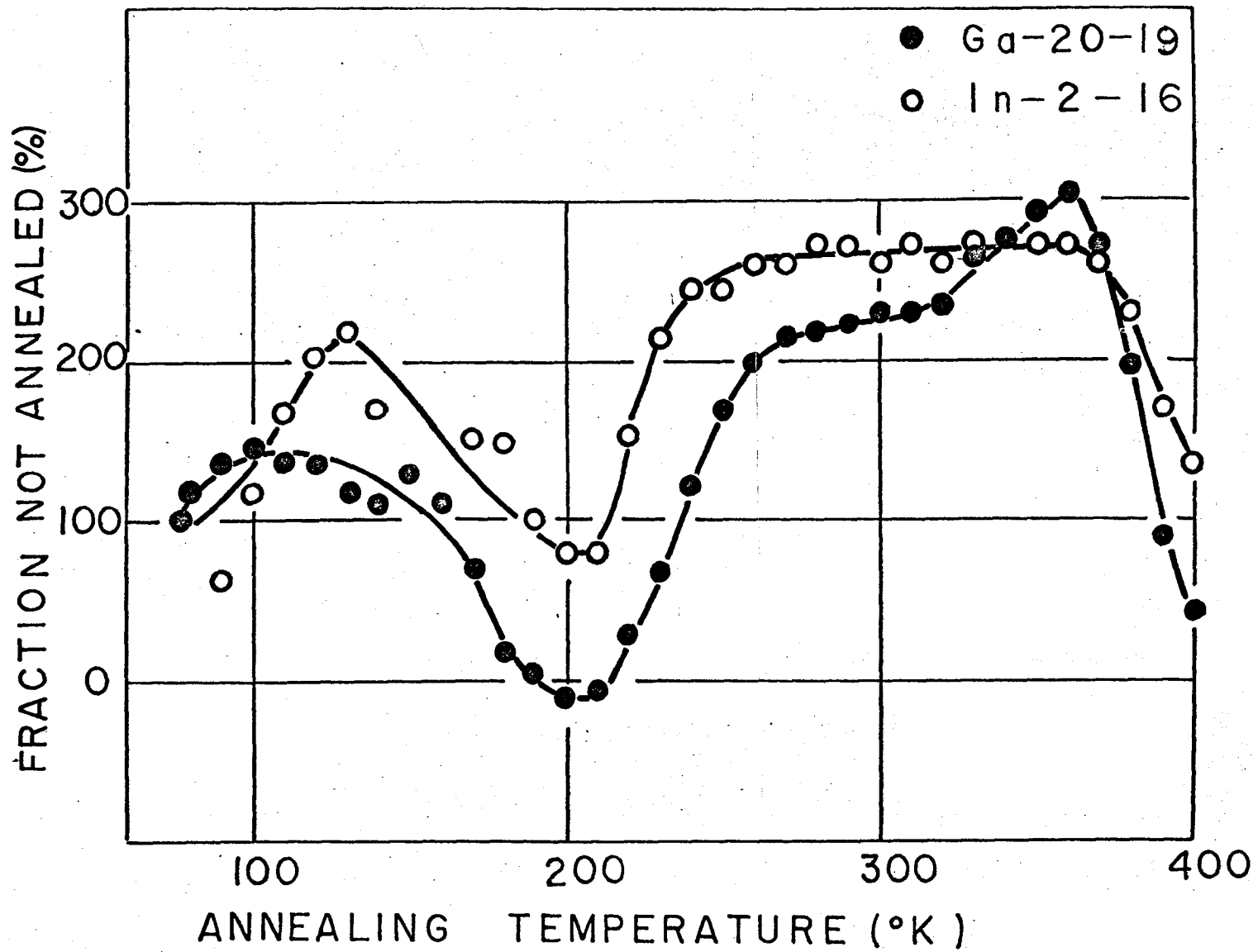


Fig. 11. 20min isochronal annealing curves of gallium-doped and indium-doped specimens. The unannealed fraction is plotted against temperature.

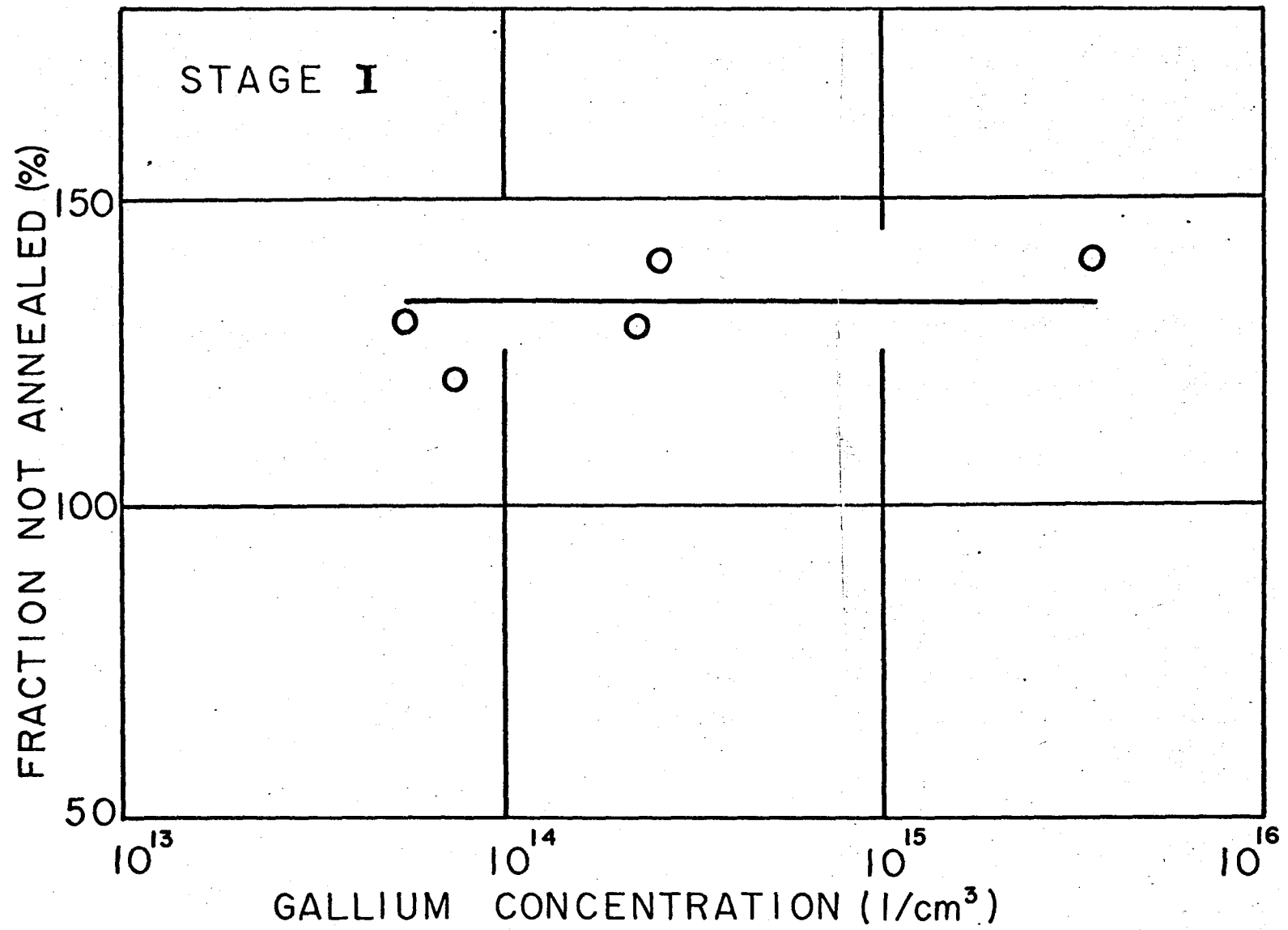


Fig. 12. Relation of the amount of the stage I and gallium concentration.

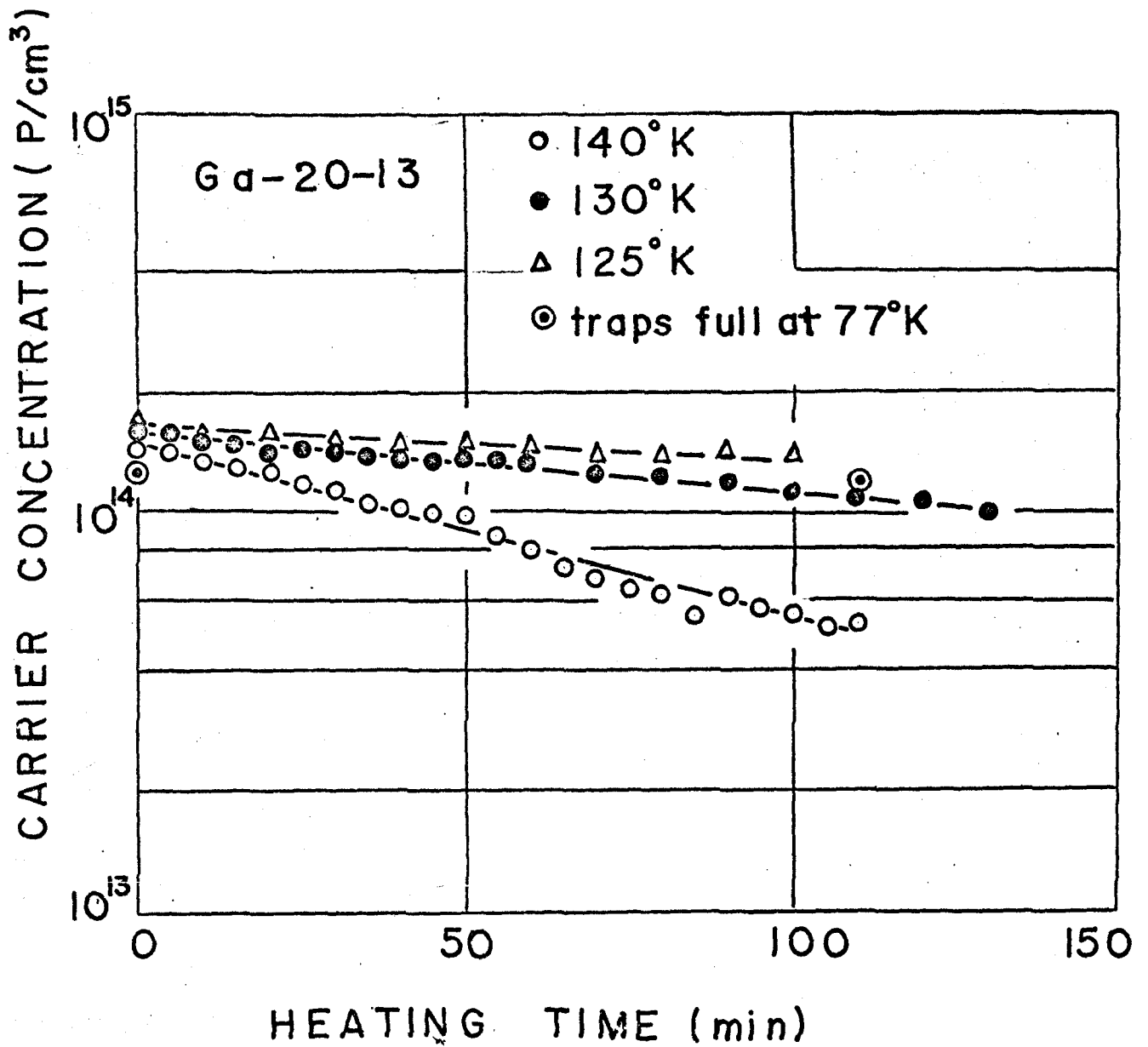


Fig. 13. Change in carrier concentration during isothermal heatings at 125°, 130° and 140°K, after isochronal anneal to 150°K.

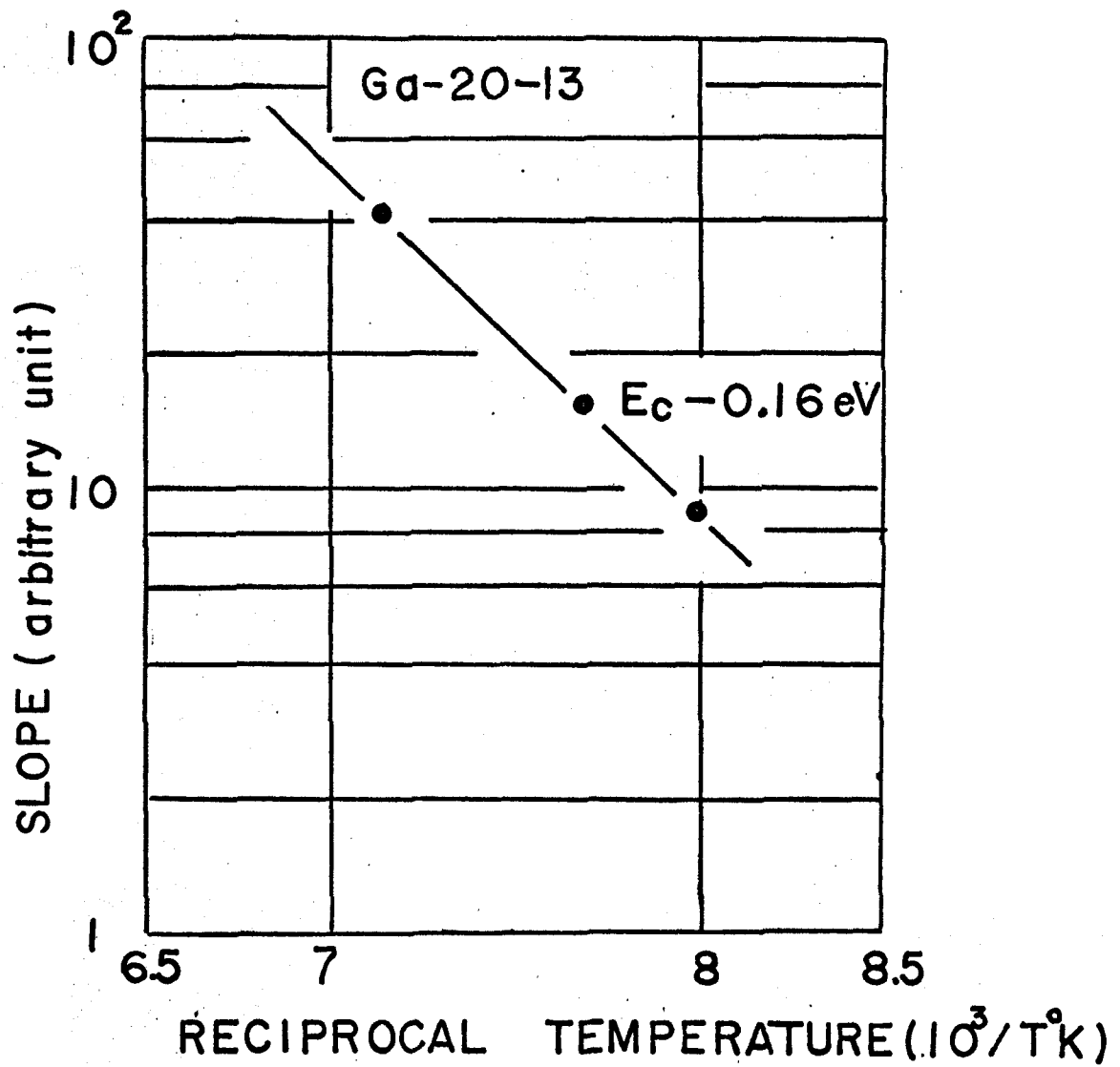


Fig. 14. Time rate of release of electrons from the shallow traps vs reciprocal temperature.



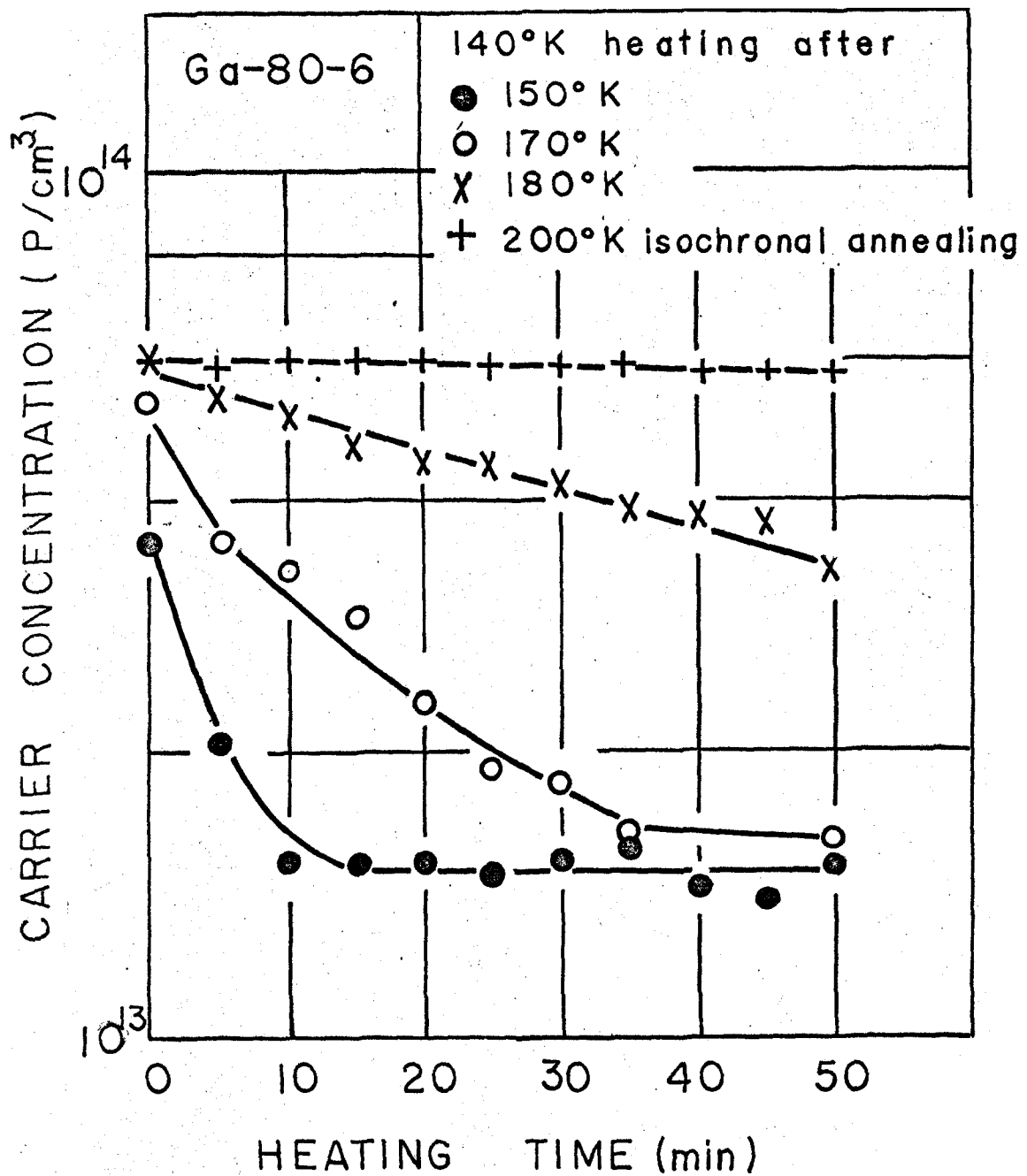
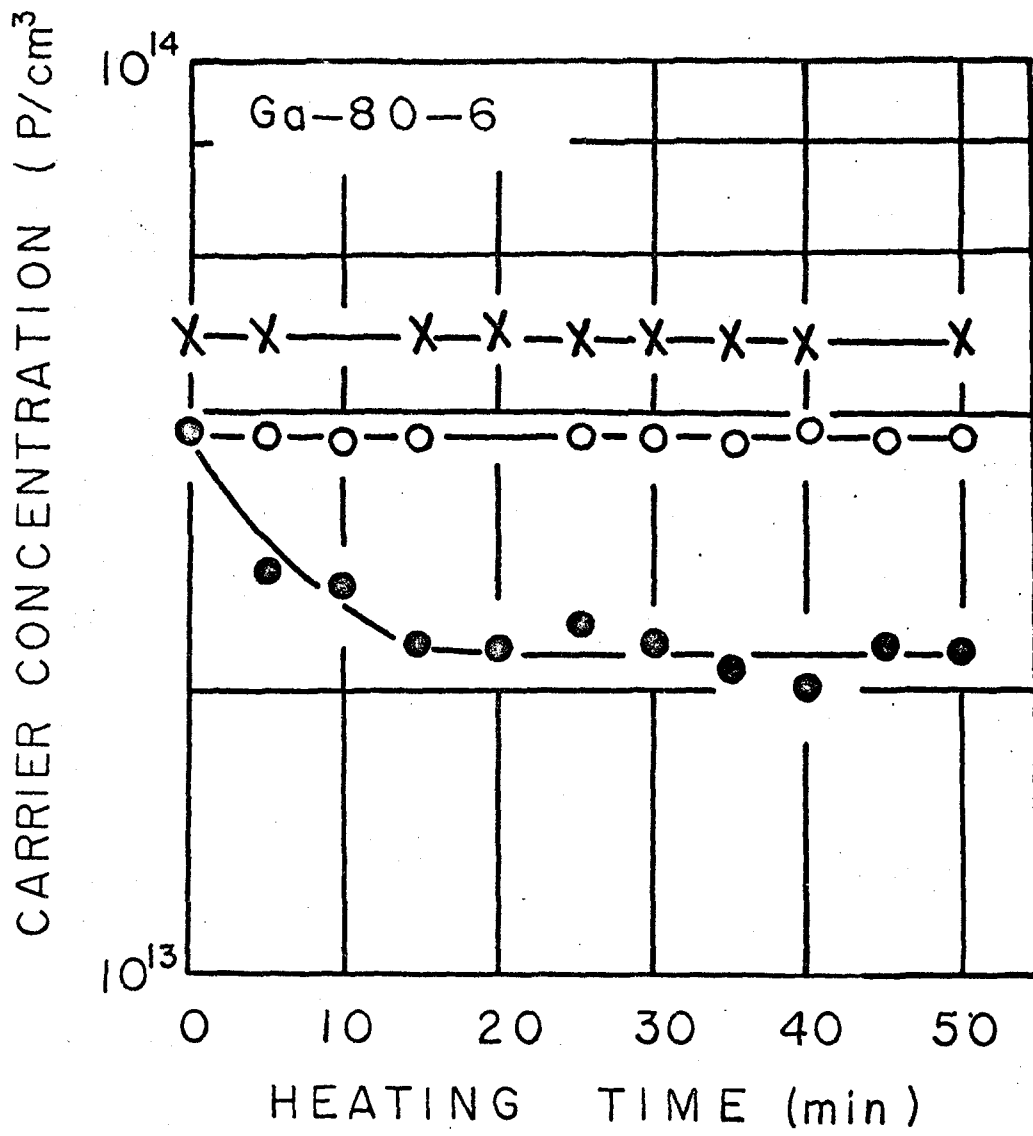


Fig. 15. Change in carrier concentration during isothermal heatings at 140°K, after the sample had been annealed to 150°, 170°, 180° and 200°K.



- 170°K heating after anneal to 230°K
- 200°K heating after anneal to 230°K
- X 170°K heating after anneal to 270°K

Fig. 16. Results of heating experiments after isochronal anneal to 230° and 270°K.

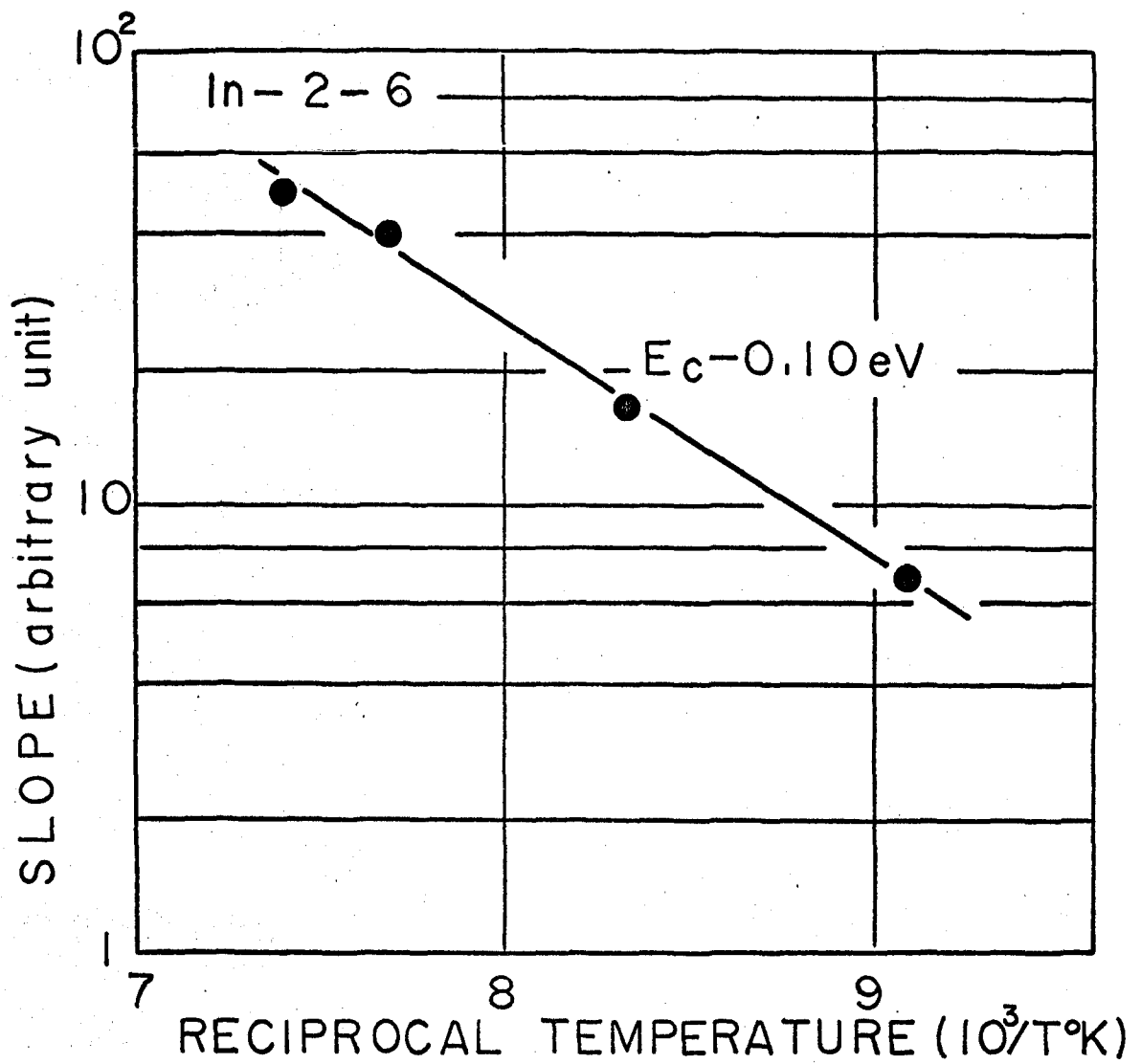


Fig. 17. Time rate of release of electrons from the shallow traps vs reciprocal temperature on indium-doped sample.

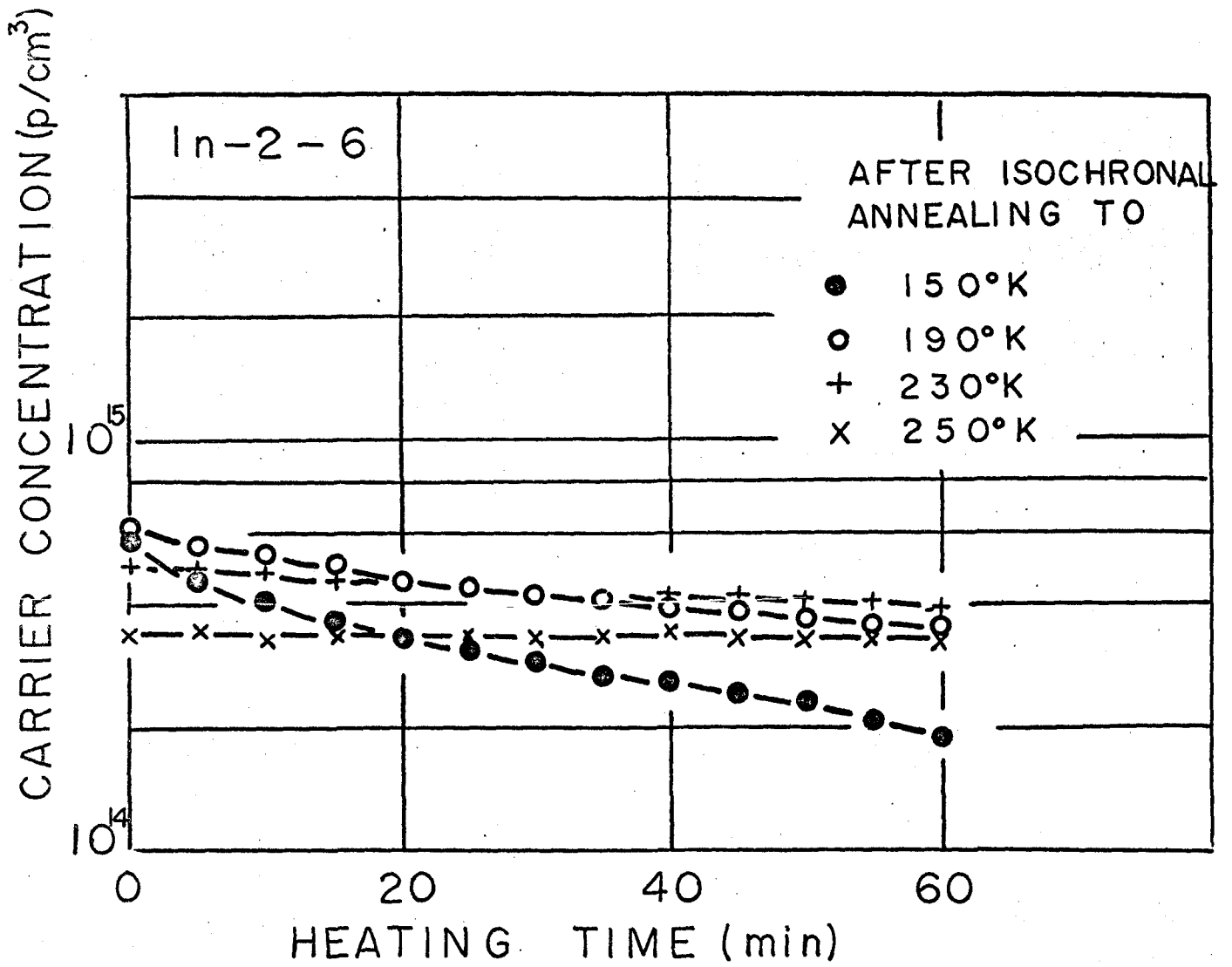


Fig. 18. Change in carrier concentration during isothermal heatings at 130°K, after isochronal anneal to 150°, 190°, 230° and 250°K in the dark.

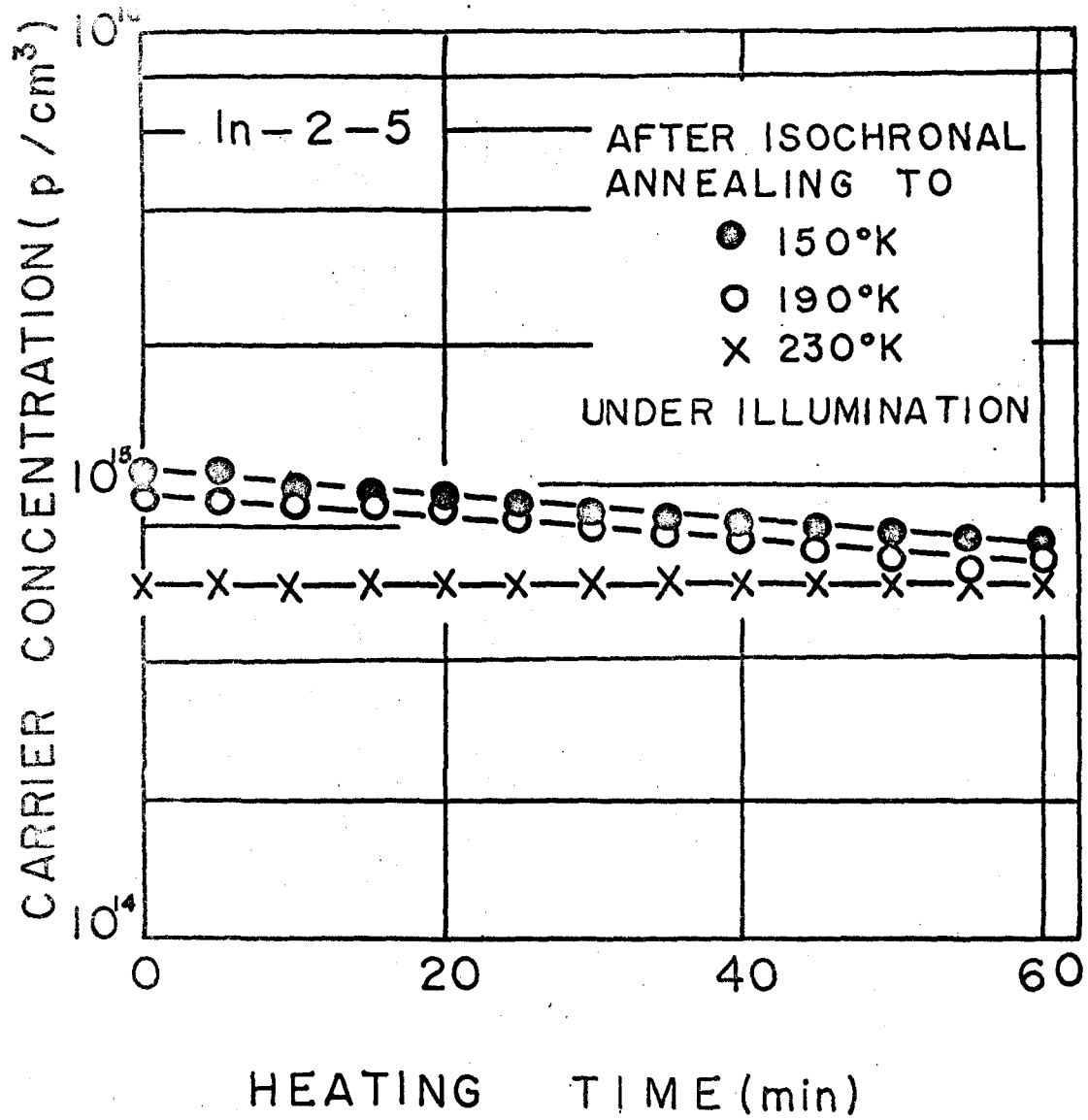


Fig. 19. Change in carrier concentration during isothermal heatings at 130°K, after isochronal anneal to 150°, 190° and 230°K in visible light.

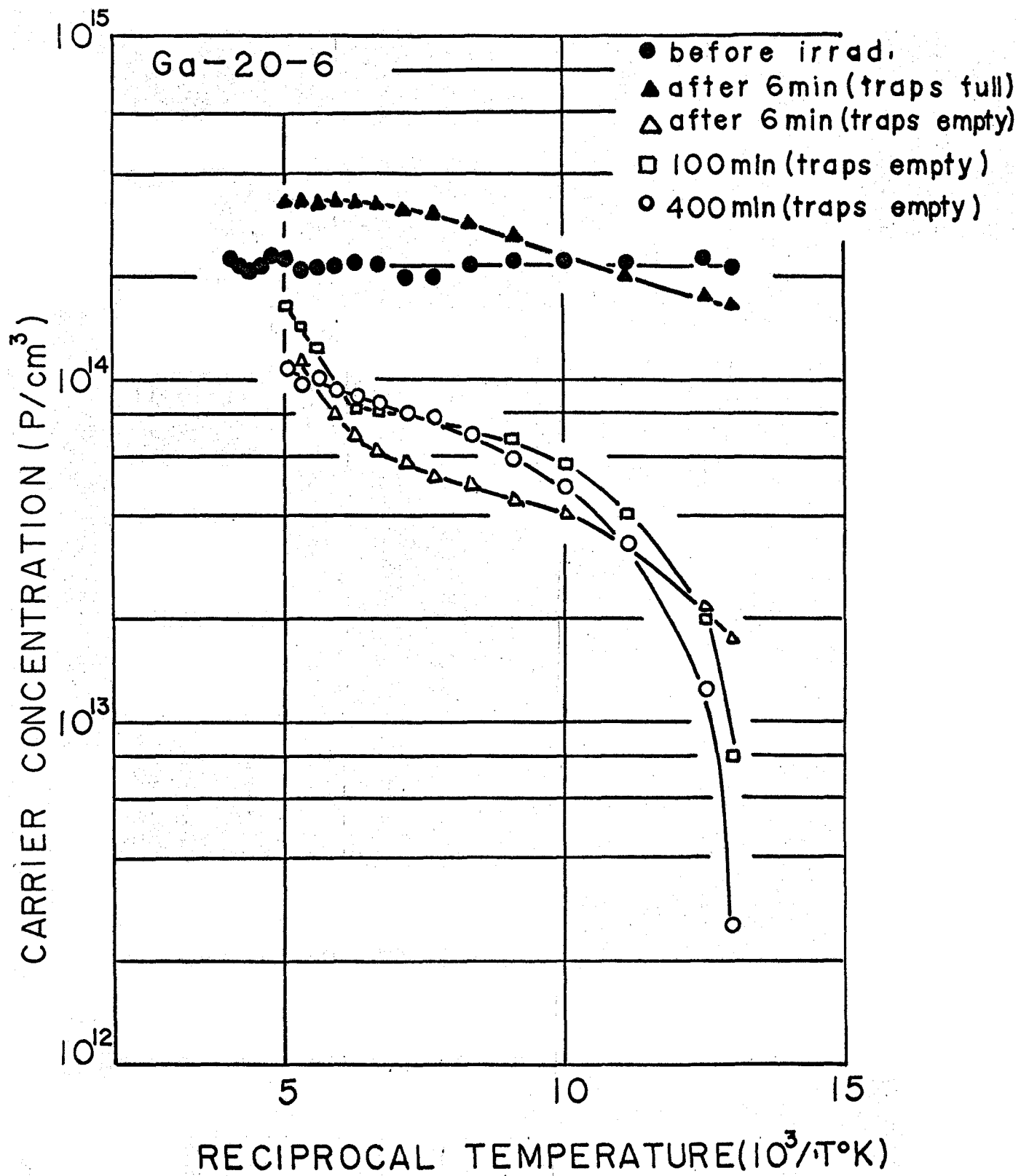


Fig. 20. Temperature dependence of carrier concentration after successive annealing at 230°K.

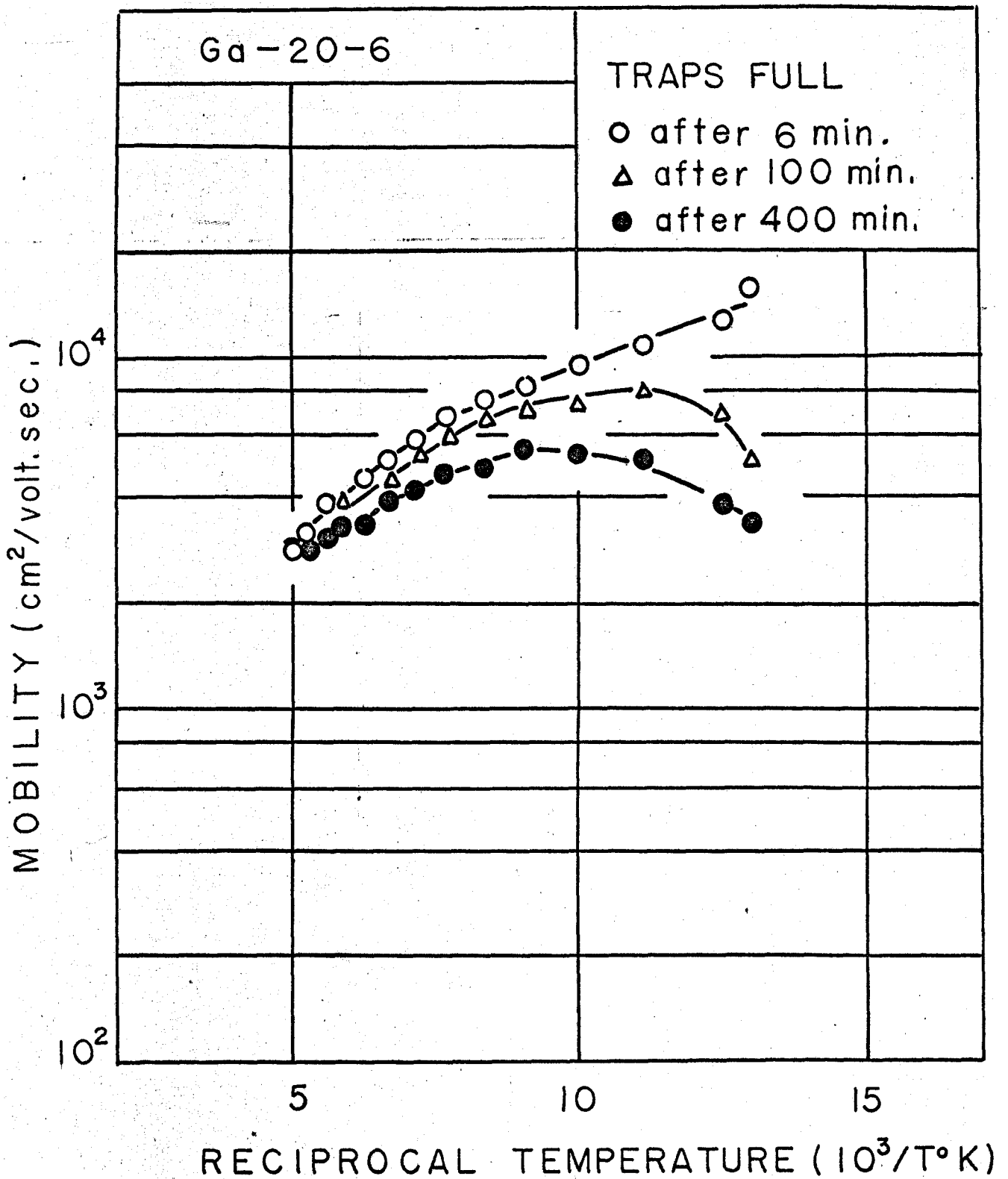
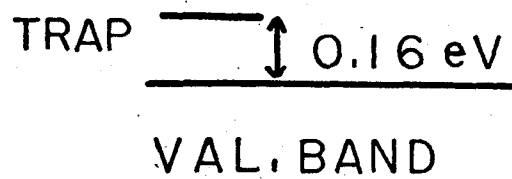
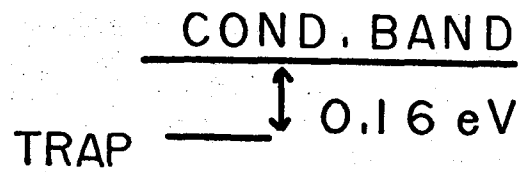


Fig. 21. Temperature dependence of mobility after successive annealing at  $230^\circ K$ .

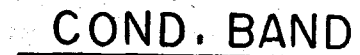


150°K



VAL. BAND

210°K



VAL. BAND

270°K

Fig. 22. Energy level scheme in irradiated gallium-doped p-type germanium.



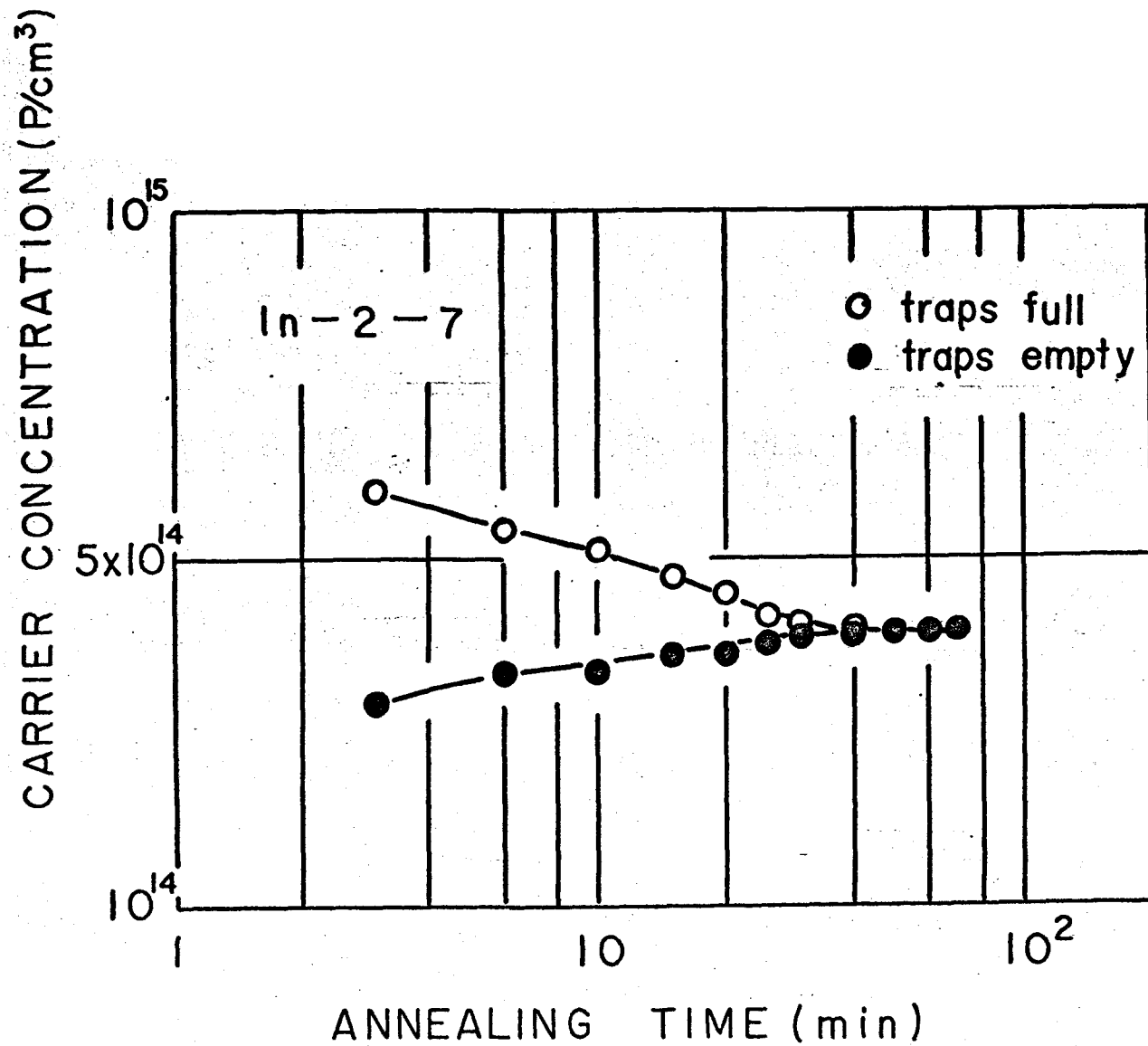


Fig. 23. Anneal of the electron traps produced by electron irradiation. Annealing is done in the dark at 250°K.

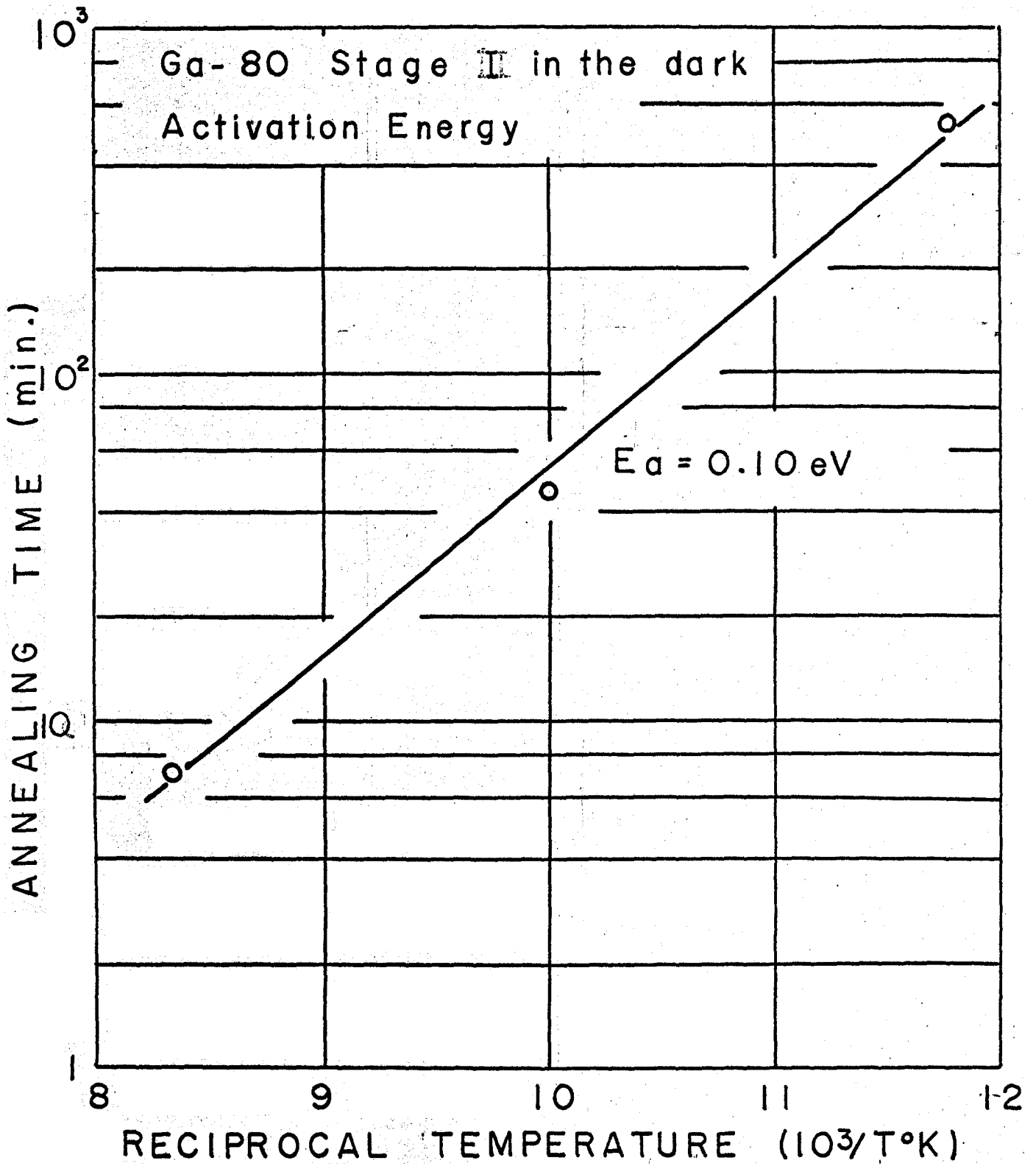


Fig. 24. Time for 50% anneal vs reciprocal temperature.

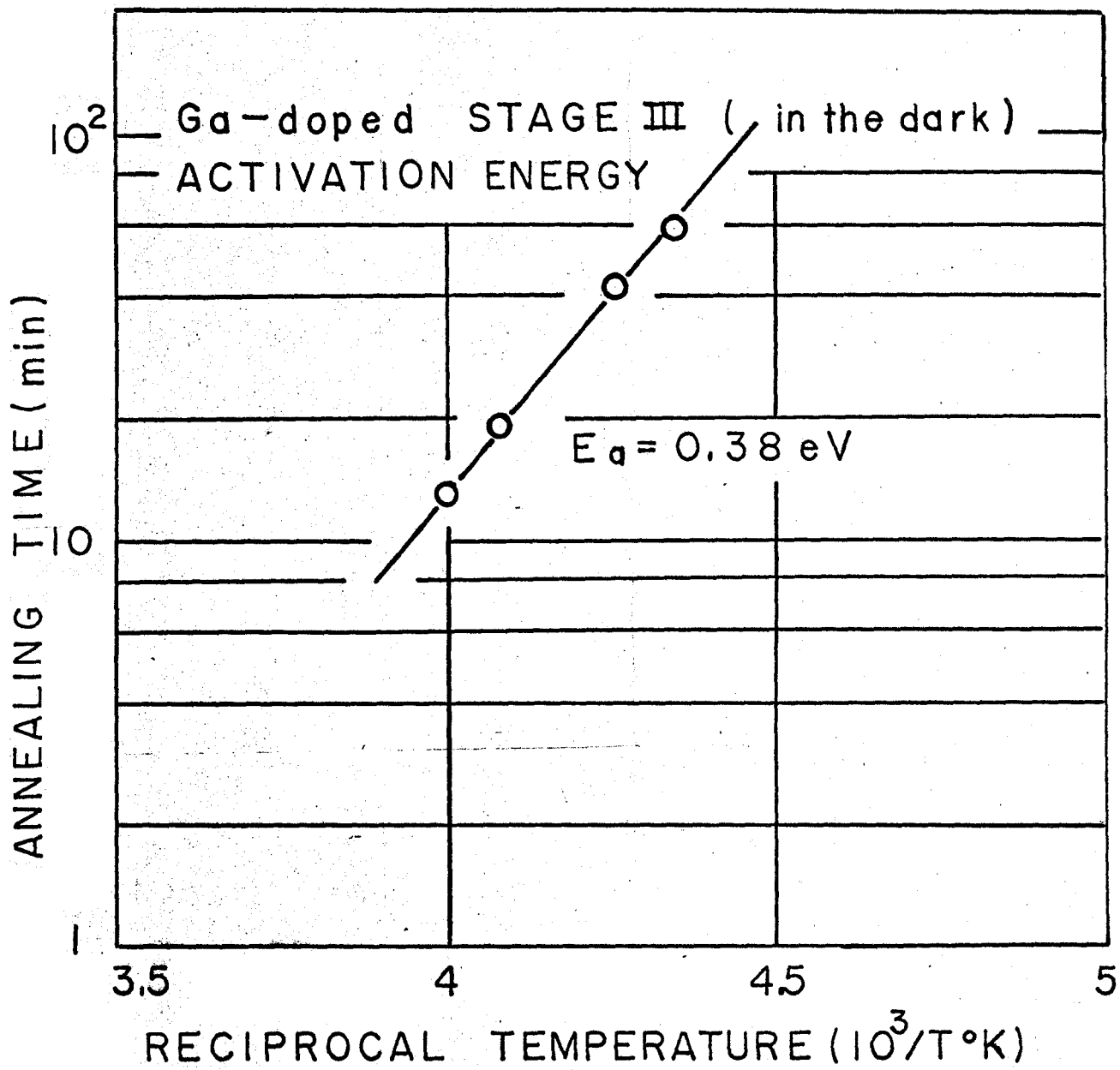


Fig. 25. Time for 50% anneal vs reciprocal temperature.

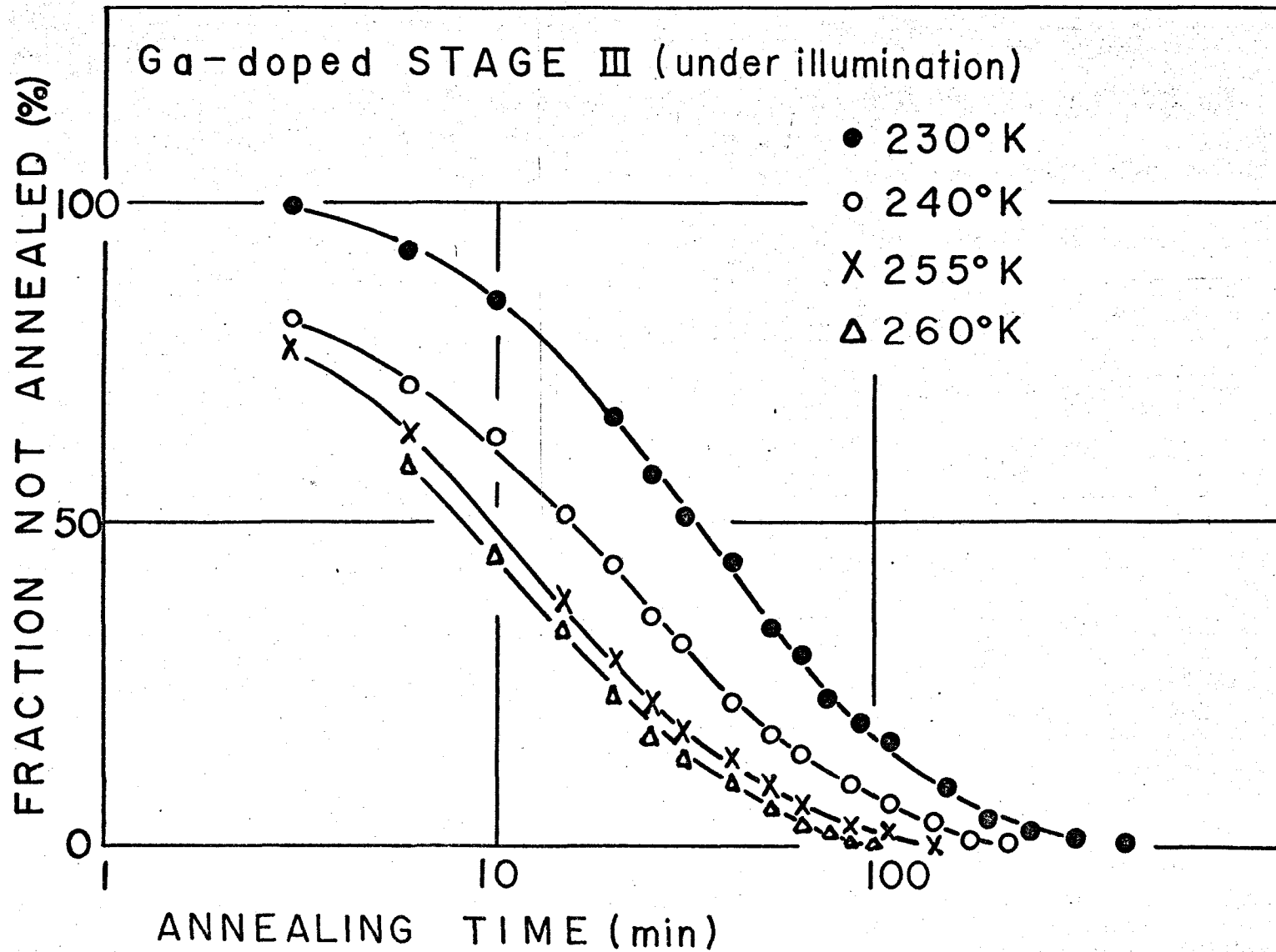


Fig. 26. Isothermal annealings of four gallium-doped specimens in visible light. The recovery was determined from carrier concentration measurements.

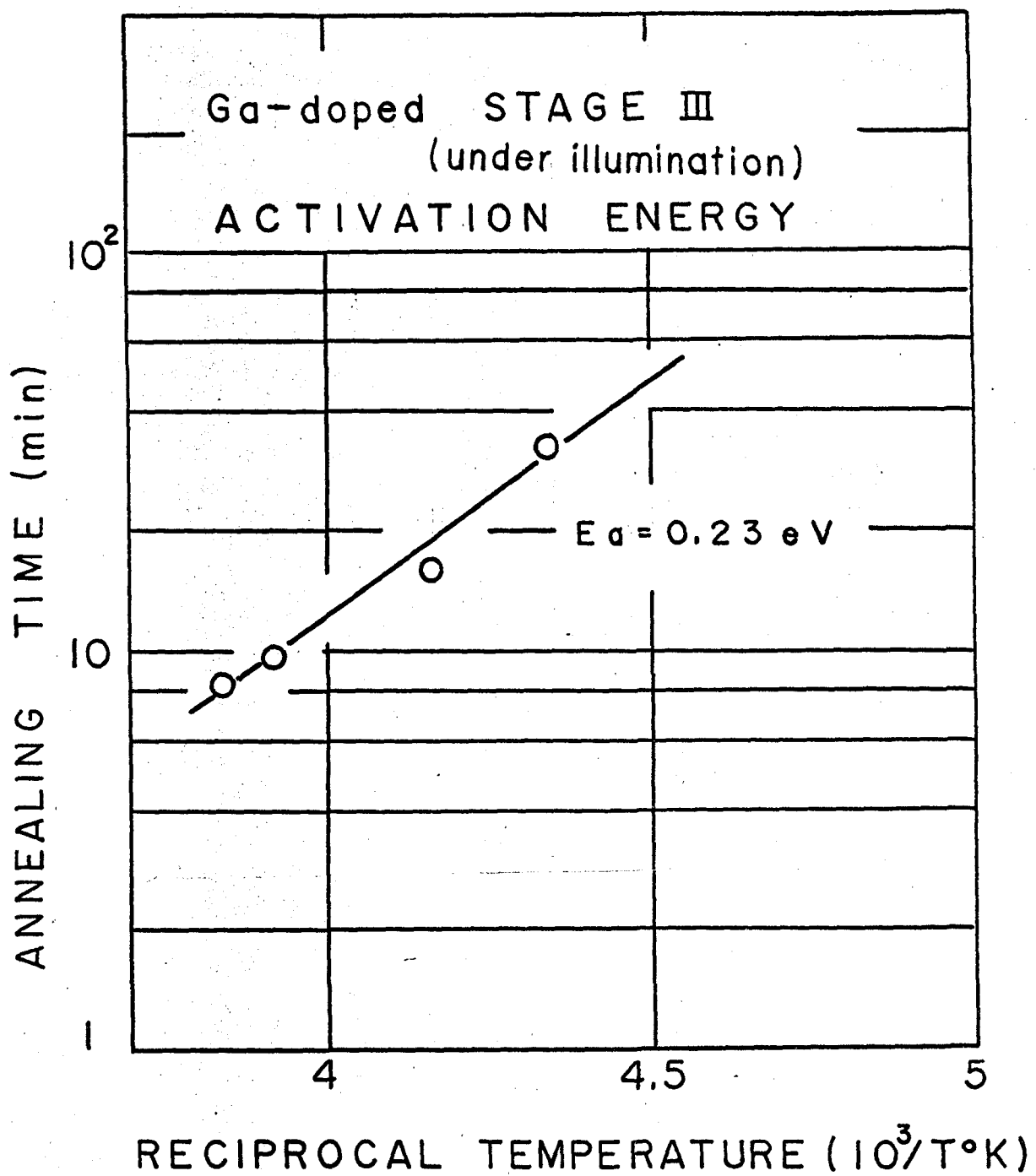


Fig. 27. Characteristic annealing times for different temperatures as shown in Fig. 26. The activation energy is 0.23eV.

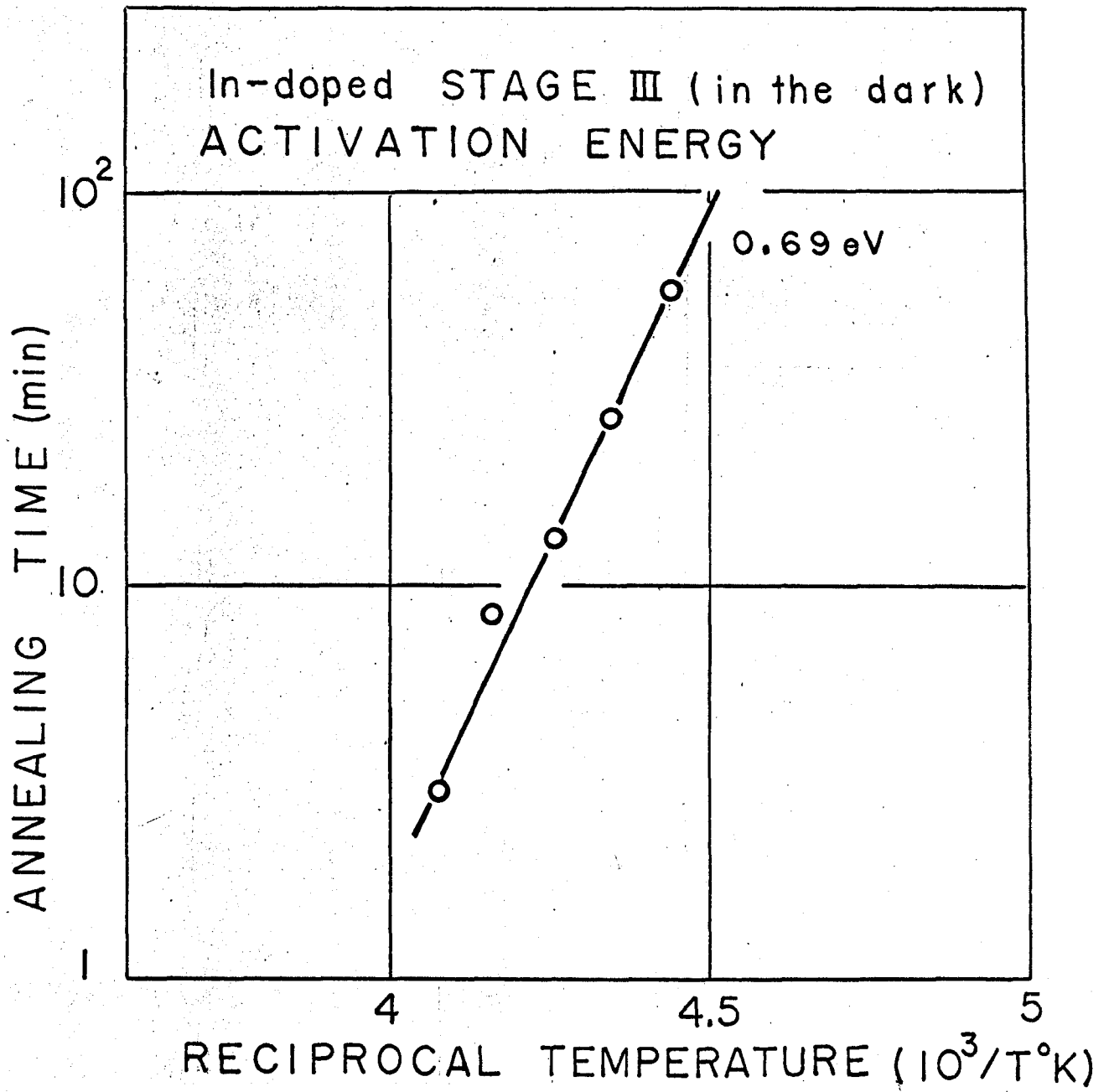


Fig. 28. Time for 50% anneal vs reciprocal temperature.

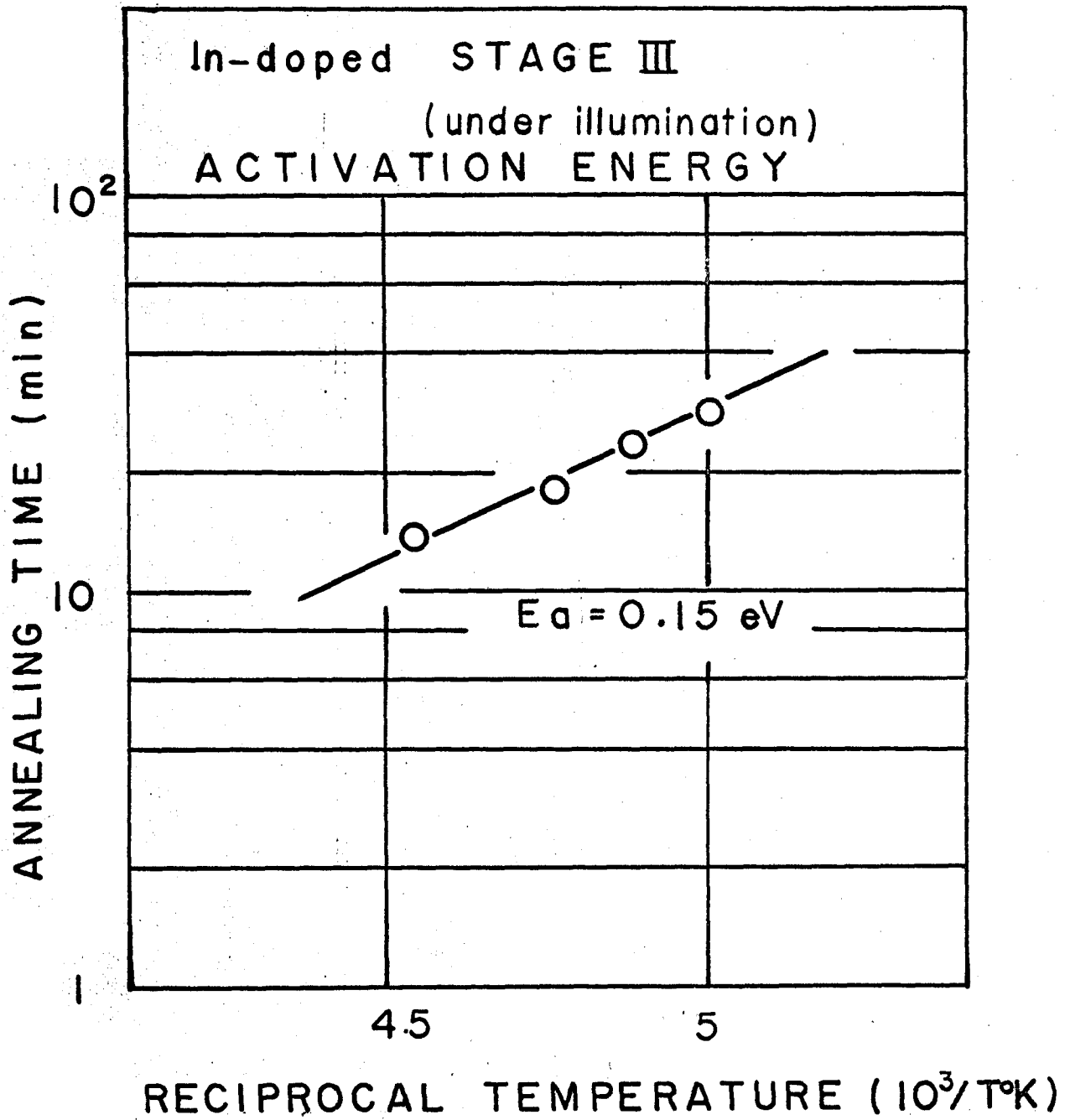


Fig. 29. Time for 50% anneal vs reciprocal temperature.

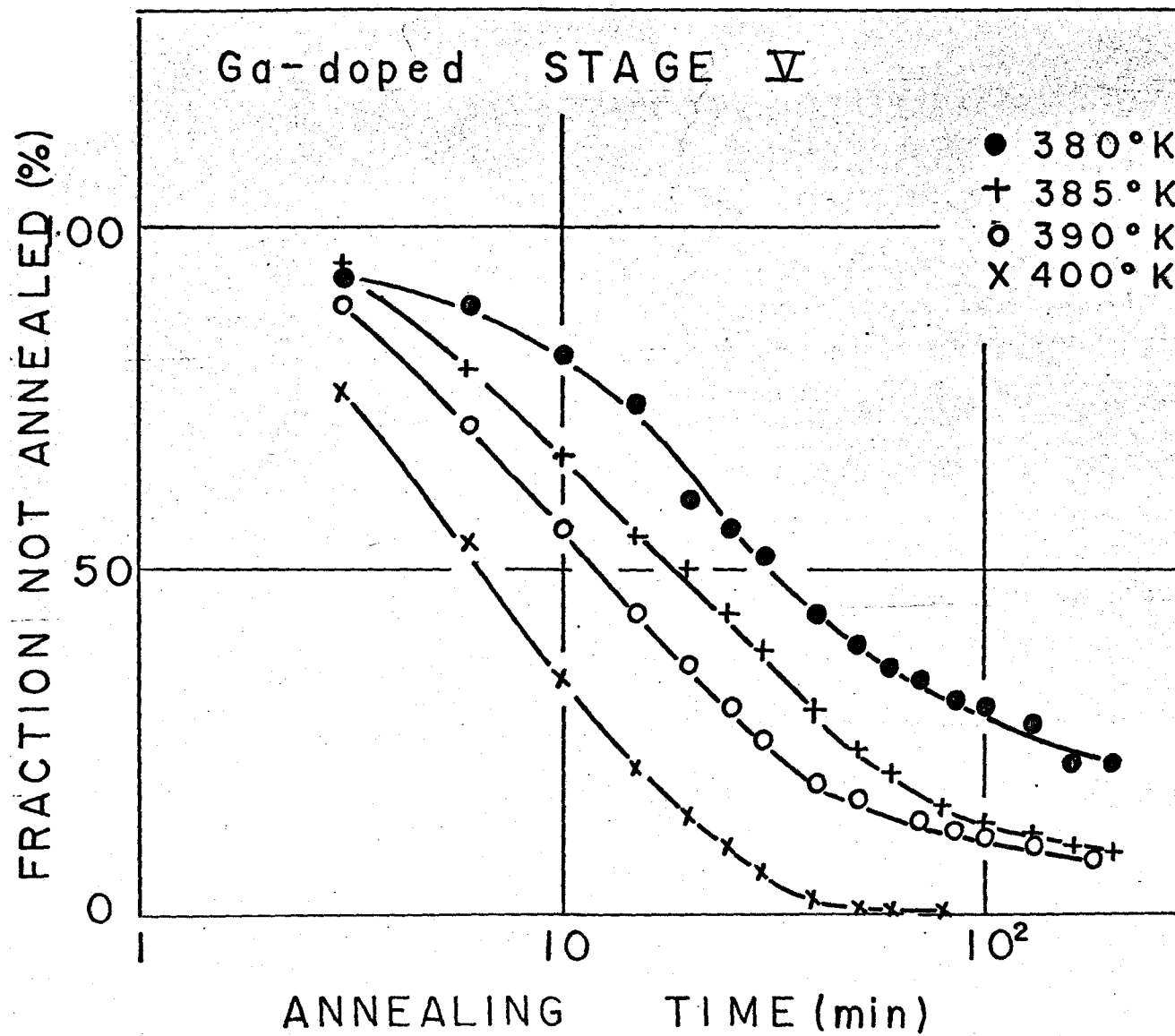


Fig. 30. Isothermal annealings of four gallium-doped specimens. The recovery was determined from carrier concentration measurements.



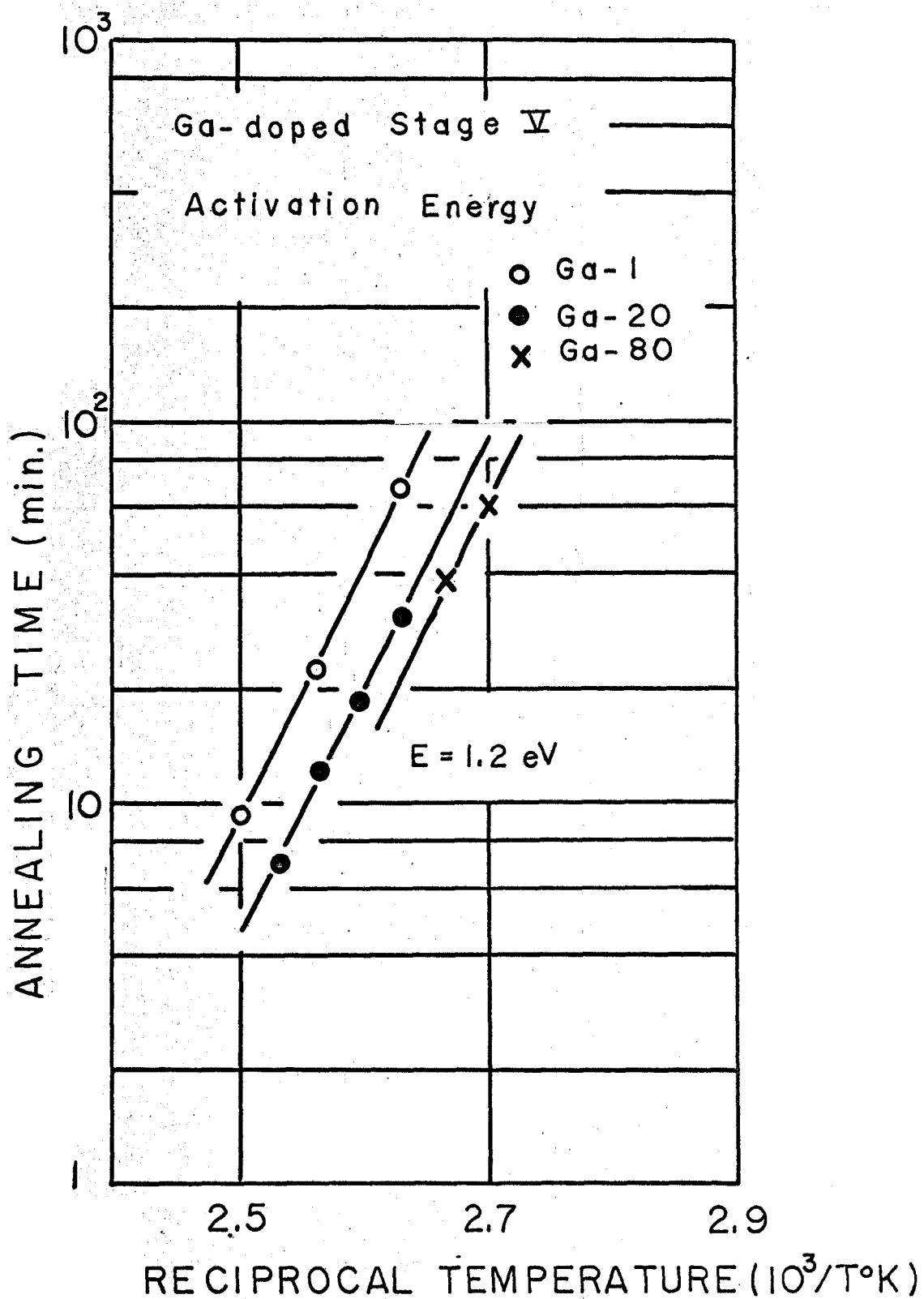


Fig. 31. Characteristic annealing times for different temperatures as shown in Fig. 30. The activation energy is 1.2eV.

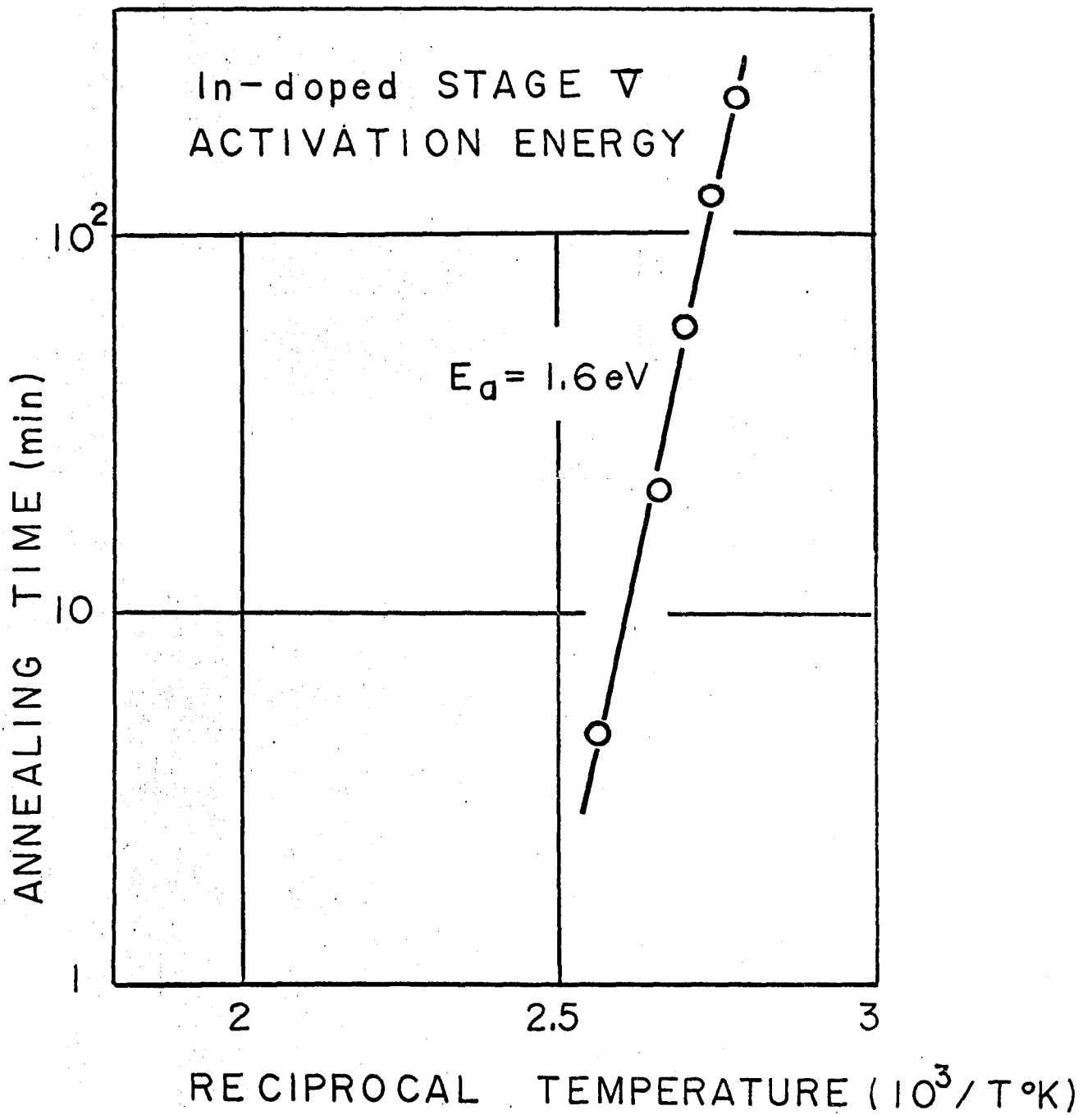


Fig. 32. Time for 50% anneal vs reciprocal temperature.

	Ga-doped			In-doped		
Stage	III		V	III		V
	traps empty	traps full		traps empty	traps full	
Act. Energy (eV)	0.38	0.23	1.2	0.69	0.15	1.6
Kinetics	1st	1 < < 2	2nd	1st	1 < < 2	2nd
Freq. Factor (1/sec.)	$5 \times 10^4$	$4 \times 10$	$10^{12}$	$10^{12}$	3	$10^{18}$

Table 1. Activation energies, kinetics and frequency factors for gallium-doped and indium-doped specimens.